Journal of Human Evolution 174 (2023) 103292

Contents lists available at ScienceDirect

Journal of Human Evolution

journal homepage: www.elsevier.com/locate/jhevol

Multi-isotope zooarchaeological investigations at Abri du Maras: The paleoecological and paleoenvironmental context of Neanderthal subsistence strategies in the Rhône Valley during MIS 3

Kate Britton [a, b, *], Elodie-Laure Jimenez [a, c], Mael Le Corre [a], Sarah Pederzani [b, d], Camille Daujeard [e], Klervia Jaouen [b, f], Delphine Vettese [e, g, h], Thomas Tütken [i], Jean-Jacques Hublin [b, j], Marie-Hélène Moncel [e]

[a] Department of Archaeology, University of Aberdeen, Aberdeen AB24 3UF, United Kingdom
[b] Department of Human Evolution, Max Planck Institute for Evolutionary Anthropology, 04103 Leipzig, Germany
[c] Royal Belgian Institute of Natural Sciences, 29 Vautier Street, 1000 Brussels, Belgium
[d] Instituto Universitario de Bio-Orgánica Antonio González, Universidad de La Laguna, Avda. Astrofísico Francisco Sánchez 2, 38206 La Laguna, Tenerife, Spain
[e] UMR 7194, Histoire Naturelle de l'Homme Préhistorique (HNHP), CNRS, Muséum National d'Histoire Naturelle, Département Homme et Environnement, Institut de Paléontologie Humaine, 1 Rue René Panhard, 75013 Paris, France
[f] Géosciences Environnement Toulouse, Observatoire Midi Pyrénées, UMR 5563, CNRS, 14 Avenue Edouard Belin, 31400 Toulouse, France
[g] Universita degli Studi di Ferrara, Dipartimento degli Studi Umanistici, Sezione di Scienze Preistoriche e Antropologiche, Corso Ercole I d'Este 32, 44121 Ferrara, Italy
[h] Grupo de I+D+i EVOADAPTA (Evolución Humana y Adaptaciones Económicas y Ecológicas durante La Prehistoria), Dpto. Ciencias Históricas, Universidad de Cantabria, Av/Los Castros 44, 39005 Santander, Spain
[i] Arbeitsgruppe für Angewandte und Analytische Paläontologie, Institut für Geowissenschaften, Johannes Gutenberg-Universität Mainz, J.-J. Becherweg 21, 55128 Mainz, Germany
[j] Collège de France, 11, Place Marcelin Berthelot, 74005 Paris, France

ARTICLE INFO

Article history:
Received 28 October 2021
Accepted 21 October 2022
Available online 29 November 2022

Keywords:
Middle Paleolithic
Collagen
Enamel
Dietary niche
Biogeography
Paleotemperatures

ABSTRACT

The exploitation of mid- and large-sized herbivores (ungulates) was central to hominin subsistence across Late Pleistocene Europe. Reconstructing the paleoecology of prey-taxa is key to better understanding procurement strategies, decisions and behaviors, and the isotope analysis of faunal bones and teeth found at archaeological sites represent a powerful means of accessing information about past faunal behaviors. These isotope zooarchaeological approaches also have a near-unique ability to reveal environmental conditions contemporary to the human activities that produced these remains. Here, we present the results of a multi-isotope, multitissue study of ungulate remains from the Middle Paleolithic site of Abri du Maras, southern France, providing new insights into the living landscapes of the Rhône Valley during MIS 3 (level 4.2 = 55 ± 2 to 42 ± 3 ka; level 4.1 = 46 ± 3 to 40 ± 3 ka). Isotope data (carbon, nitrogen) reveal the dietary niches of different ungulate taxa, including the now-extinct giant deer (*Megaloceros*). Oxygen isotope data are consistent with a mild seasonal climate during level 4.2, where horse (*Equus*), bison (*Bison*), and red deer (*Cervus elaphus*) were exploited year-round. Strontium and sulfur isotope analyses provide new evidence for behavioral plasticity in Late Pleistocene European reindeer (*Rangifer*) between level 4.2 and level 4.1, indicating a change from the migratory to the sedentary ecotype. In level 4.1, the strong seasonal nature of reindeer exploitation, combined with their nonmigratory behavior, is consistent with a seasonally restricted use of the site by Neanderthals at that time or the preferential hunting of reindeer when in peak physical condition during the autumn.

* Corresponding author.
E-mail address: k.britton@abdn.ac.uk (K. Britton).

https://doi.org/10.1016/j.jhevol.2022.103292

1. Introduction

1.1. Context

The exploitation of mid- and large-sized herbivores was a key adaptive behavior of both Neanderthal and early *Homo sapiens* across north-west Europe throughout the Middle and Late Pleistocene (Discamps et al., 2011; Kuntz and Costamagno, 2011; Rendu et al., 2012; Marín et al., 2020). Reconstructing the paleoecology of prey-taxa is vital to better understanding hominin procurement strategies, decisions, and behaviors. While the Last Glaciation (Marine Isotope Stage [MIS] 4–2; ~74–12 ka) was marked by climate fluctuations, MIS 3 (~57–29 ka) was a period of profound climatic instability, characterized by short-term and acute climatic oscillations (Voelker, 2002; Barron et al., 2003; Lisiecki and Raymo, 2005; Clement and Peterson, 2008; Kindler et al., 2014). Although long-term species distribution and turnover is generally well characterized in the Late Pleistocene (Kahlke, 2014; Puzachenko et al., 2020), the impact contemporary climatic changes would have had on the behaviors of ungulate species is less well known, and the relationships between rapid climatic shifts and the dietary and migratory behaviors of ungulate species are poorly characterized. In turn, the interactions between changes in prey-species behavior and hominin subsistence strategies can be difficult to elucidate. There is a clear need for site-specific approaches, where the reconstruction of local environmental and paleoecological conditions can be contrasted to archaeological evidence to gain more nuanced interpretations of the interactions between environmental dynamism, the behaviors of prey-species and the subsistence strategies and landscape use of early human groups.

In recent decades, the stable isotope analysis of zooarchaeological assemblages has emerged as a leading means of reconstructing past faunal paleoecology, paleoenvironments, and paleotemperatures. Carbon and nitrogen isotope ratios of bone collagen derive from diet, and in modern ecosystems and recent historic case studies have been shown to reflect both broad environmental conditions and also the niche feeding behaviors of different taxa of large herbivores over the period of tissue formation (e.g., Ben-David et al., 2001; Drucker et al., 2001, 2012; Feranec, 2007; Hofman-Kamińska et al., 2018). Sulfur isotope ratios measured in bone collagen can also prove useful in food web studies but when considering ungulate species are of most use as a tool for reconstructing geographical range use, with values corresponding to local soils and lithological unit, rainfall, and coastal proximity (see review in Nehlich, 2015). As strontium isotope ratios of skeletal tissues relate directly to that of local lithology, soils and plants, these techniques can provide more direct evidence of movement histories (see Britton, 2020, for an overview). When combined with the serial sampling of incrementally developing tissues that do not undergo subsequent remodeling, such as tooth enamel (Hillson, 2005), these can provide evidence of time-series (i.e., seasonal) movement information, as demonstrated in modern migratory North American caribou (Britton et al., 2009). Given the relationship between temperature and the $\delta^{18}O$ value of local precipitation, and the near-linear relationship between the $\delta^{18}O$ value of body water and that of mineralized tissues, the oxygen isotope analysis of mammalian skeletal tissues can provide valuable insights into past thermal conditions (see Pederzani and Britton, 2019, for an overview). When obligate drinking species, such as horses or bison, are targeted and sequential sampling approaches are used (i.e., of molariform teeth), these approaches can provide evidence of local seasonal climatic conditions (Fricke et al., 1998; Kohn et al., 1998; Sharp and Cerling, 1998). These techniques have successfully been applied to European Middle and Late Pleistocene sites, reconstructing paleoclimate and paleoenvironmental change, faunal niche feeding behaviors and migratory habits, and through this better understanding hominin subsistence strategies (e.g., Bocherens, 2003; Richards and Hedges, 2003; Stevens and Hedges, 2004; Pellegrini et al., 2008; Stevens et al., 2008; Bernard et al., 2009; Fabre et al., 2011; Britton et al., 2011, 2012, 2019; Price et al., 2017; Drucker et al., 2018; Jones et al., 2018, 2019; Schwartz-Narbonne et al., 2019; Drucker, 2022).

1.2. Reconstructing faunal paleoecology and paleoenvironmental conditions using isotope zooarchaeology

The isotopic compositions of preserved faunal tissues found at archaeological and paleontological sites, including dental enamel and collagen extracted from bones, are a complex product of isotopic inputs during life and the biological process that occur within an organism. Given the variation inherent in many different isotopic systems across landscapes and between (and within) biomes, isotopic inputs obtained through food and water ingested reflect feeding behaviors but also prevailing environmental conditions and geospatial histories, as well as an organism's physiology. Understanding these issues, and the fundamental principles, assumptions, and caveats inherent behind the application of these isotopic techniques to mammalian tissues, is essential in order to be able to interpret isotopic data from zooarchaeological and paleontological remains.

Carbon isotopes Carbon isotope techniques are based on the principle that animal body tissues (e.g., bone collagen) reflect the isotopic composition of the food ingested throughout life. The relative abundance of the stable isotopes of carbon, ^{13}C and ^{12}C ($\delta^{13}C$), varies characteristically between different biomes—for example, between plants of different photosynthetic pathways (Smith and Epstein, 1971; DeNiro and Epstein, 1978) or between terrestrial and marine ecosystems (Schoeninger and DeNiro, 1984). Studies of resource partitioning and niche feeding ecology have generally focused on environments where both C_3 and C_4 plants can be found, such as subtropical Africa (e.g., Koch et al., 1995; Cerling et al., 1999) and North America (e.g., Gadbury et al., 2000; MacFadden, 2008). These plants have different photosynthetic pathways, selecting against ^{13}C to different degrees, and therefore display large differences in their $\delta^{13}C$ values. However, studies have demonstrated the effectiveness of carbon isotope analysis to reveal resource partitioning among modern (e.g., Feranec, 2007; Hofman-Kamińska et al., 2018) and Late Pleistocene (e.g., Britton et al., 2012; Schwartz-Narbonne et al., 2019) ungulates in purely C_3 environments. Such variations stem from intraecosystem variations in carbon isotope values of different plant communities and reflect dietary choices of herbivores living within C_3 environments (see Bocherens, 2003; Drucker, 2022, for an overview). Lichens, for example, exhibit less negative $\delta^{13}C$ values than other terrestrial plants incorporated into the diet of Northern ungulates (Park and Epstein, 1960; Maguas and Brugnoli, 1996; Ben-David et al., 2001). This has been demonstrated to raise ^{13}C amounts in the blood and dentine of modern *Rangifer* (Ben-David et al., 2001; Drucker et al., 2001), and is often reflected in bone collagen $\delta^{13}C$ values of Late Pleistocene European *Rangifer* (e.g., Fizet et al., 1995). Closed forest systems, including temperate woodlands (Bonafini et al., 2013), can feature anomalously ^{13}C-depleted vegetation, a so-called 'canopy effect.' Anticipated differences between the bone collagen $\delta^{13}C$ values of a species regularly feeding on lichens or in dense forest have therefore formed the basis of investigations in cervid feeding ecology in Late Pleistocene Europe, inferring both niche partitioning but also broader environmental conditions (e.g., Drucker et al., 2008; Immel et al., 2015). It should also be noted that the $\delta^{13}C$ values of bodily proteins can also reflect physiological differences, such as ruminant digestion and methane production,

which leads to tissue ^{13}C-enrichment (e.g., Cerling and Harris, 1999).

While δ^{13}C values can also be obtained from the carbonate component of dental enamel, where preservation permits, bone collagen is often the favored analyte in studies of faunal dietary paleoecology as (due to remodeling and renewal) it reflects averaged dietary isotopic intake over a number of years (e.g., Hedges et al., 2007) and the preservation and isotopic integrity of bone collagen can be assessed using several quality indicators (DeNiro, 1985; van Klinken, 1999). Furthermore, analysis of bone collagen often permits the cogeneration of nitrogen and, increasingly, also sulfur isotope data, which can aid in the inference of other aspects of faunal paleoecology.

Nitrogen isotopes The δ^{15}N values of ungulate bone collagen depends on several factors, most notably the δ^{15}N values of the plants at the base of the food chain. A range of variables can lead to depletion or enrichment in plant ^{15}N, which, in turn, could affect the tissue δ^{15}N values of animal feeders. Plant δ^{15}N values depend on nitrogen availability, the source of nitrogen that is incorporated into the plant, the characteristics of nitrogen cycling in the soils at any given location, as well the plant's physiology in terms of how they uptake nitrogen (Högberg, 1997; Amundson et al., 2003; Hobbie and Högberg, 2012). Plants that obtain their nitrogen with the assistance of mycorrhizae, for example, tend to have lower δ^{15}N values than plants that lack these symbionts (Högberg 1997). This means that in contemporary arctic and boreal ecosystems, grasses—which do not obtain their nitrogen with the assistance of these fungal associations—are normally ^{15}N-enriched relative to shrubs and trees that do (see data collated in Bocherens, 2003: 61, Figure 3). In environments that are extremely nutrient-poor, such as tundra environments, competitive partitioning of the overall nitrogen pool by plants through a variety of mechanisms can lead to variations in δ^{15}N values of plant species (Nadelhoffer et al., 1996). In light of these variations, selective feeding on particular plant species can lead to variation in bone collagen δ^{15}N among large herbivores, interpreted as evidence of niche partitioning in Late Pleistocene studies (e.g., Bocherens, 2003; Britton et al., 2012; Schwartz-Narbonne et al., 2019).

Large-scale studies of soil δ^{15}N values have observed trends with both temperature and precipitation (e.g., Amundson et al., 2003), and it is thought that these likely influence soil (and therefore plant) δ^{15}N values in nonagricultural (i.e., unmanaged) landscapes primarily through influencing the loss mechanisms which are part of the natural cycling of nitrogen within soils (Houlton and Bai, 2009). In contemporary ecosystems, cooler and wetter conditions influence nitrogen cycling in soils, leading to less ^{14}N being lost through leaching, denitrification, and ammonia volatilization, and thus decreasing plant δ^{15}N values (Amundson et al., 2003). Soil maturity has also been linked to ^{15}N-enrichment in plants, and plants growing on pioneer soils may have lower δ^{15}N values because of the inhibition of microbial activity (e.g., Hobbie et al., 1998). It is largely based on these broad relationships between climatic conditions and precipitation, and the pattern of glacial–interglacial successions in the Quaternary, that long-term changes in the δ^{15}N values of archaeological herbivore collagen throughout the Late Pleistocene of northwest Europe have been explained (e.g., Richards and Hedges, 2003; Stevens and Hedges, 2004; Stevens et al., 2008).

However, in modern ecosystems, although there are general trends with climate, correlations between soil/plant δ^{15}N values and climate on a global level are poor (Hobbie and Högberg, 2012). It is likely that confounding factors, such as mycorrhizal association and type, along with precipitation are perhaps the most important influences (Hobbie and Högberg, 2012). Other extraneous influences are also known to influence soil δ^{15}N values, such as grazing pressure, which can serve to raise δ^{15}N values in soils and therefore plants, in a complex cycle of nitrogen transfer between herbivores and their forage (e.g., Sjögersten et al., 2010). Bone collagen δ^{15}N values of large herbivores from the Late Pleistocene are therefore a product of multiple influences, from soil maturity and broad-scale climatic influences, to precipitation patterns, through to the individual plant communities and density of animals grazing regularly at a specific location. Furthermore, when considering the δ^{15}N values of large herbivores, potential influences of their adaptive biology and physiology on tissue δ^{15}N values must also be considered. For example, modern studies have demonstrated that ^{15}N-enrichment from diet to tissue is dependent on the protein content of graze and forage consumed, with low protein diets leading to lower diet-tissue offsets and thus (potentially) lower tissue δ^{15}N values (Sponheimer et al., 2003). Furthermore, physiological variations, such as pregnancy, lactation, and malnutrition, have also been demonstrated to influence ^{15}N-enrichment in contemporary forming tissues (e.g., Fuller et al., 2004, 2005; Mekota et al., 2006).

Sulfur isotope analysis Although data are also typically obtained from bone collagen in archaeological case studies, compared to carbon and nitrogen isotope studies there have been comparatively few applications of sulfur isotope analysis (δ^{34}S) to Late Pleistocene materials, although applications are increasing. While useful in archaeology for exploring other aspects of personal life history, such as diet (see review in Nehlich, 2015), when applied to Late Pleistocene ungulate remains, sulfur isotope analysis is perhaps most useful as a means of investigating geographical range use and, by inference, faunal spatial paleoecology and even the hunting territories of human groups (e.g., Jones et al., 2019).

At the base of the food chain, the sulfur incorporated into food webs originates from sulfates in groundwater and rain, as well as from atmospheric deposition, leading to variations in plant, and therefore herbivore, δ^{34}S values. Other sources of sulfur also contribute to the bioavailable pool (that which is incorporated into biomolecules), however, notably due to the weathering of sulfur-bearing minerals into soils from different rock types which can introduce additional variation in terrestrial contexts (see discussion in Nehlich 2015: 4, Figure 3). Another major source of variability in sulfur 'isoscapes' is coastal proximity. Sea spray sulfates result in rain and aerosols with δ^{34}S values of ~20‰ (Nielsen, 1974), a uniform and relatively high value that is distinct from the more variable values found in terrestrial and freshwater ecosystems (Peterson and Fry, 1987; Nehlich 2015). The influence of these oceanic sulfates on the δ^{34}S values of soils, plants, and animals can extend tens of kilometers in land—the 'sea spray effect' (e.g., Richards et al., 2001; Zazzo et al., 2011). Although there have been comparatively few applications (to either modern or ancient ecosystems), δ^{34}S has been applied to faunal tissues to explore migratory behavior. For example, given the distinctions between terrestrial and marine sulfates, δ^{34}S values of otoliths have been used to differentiate between anadromous and nonanadromous ecotypes of fish (e.g., Godbout et al., 2010). The sampling of modern mammalian bodily proteins such as keratin has also demonstrated strong geographical trends, especially with coastal proximity, suggesting spatial variation in sulfur isotopes may prove a useful means of exploring past faunal spatial ecology in certain contexts (e.g., Zazzo et al., 2011). Few modern studies have incorporated the analysis of sulfur isotopes in bone collagen to explore the usefulness of this approach in inferring faunal movements, although limited work on modern North American *Rangifer* and *Bison* has demonstrated differences between migratory and nonmigratory individuals, and correlations between δ^{34}S values and strontium isotope ratios (Britton, 2010).

Applications to Late Pleistocene faunal samples have indicated the potential of these techniques to infer (at least relative) differences in range use by different species in the same region (e.g., Wißing et al., 2019: 4, Figure 2) and possible changes in human hunting range utilized and/or the spatial paleoecology of prey-species through time (e.g., Jones et al., 2019). However, other studies of Late Pleistocene fauna have also indicated that faunal $\delta^{34}S$ values, via the $\delta^{34}S$ values of soils and plants, may (like $\delta^{15}N$ values) be strongly influenced by prevailing climatic conditions. This includes temperature and the presence of permafrost, both of which may serve to influence the rate of mineralization and volatilization of sulfur in soils, altering soil $\delta^{34}S$ values (e.g., Drucker et al., 2011; Reade et al., 2020). Although work is required to characterize this relationship, variability in soil $\delta^{34}S$ values induced by climatic change poses a challenge to the further development of this method as a tracer of past faunal spatial behaviors, especially in diachronic studies. The potential for baseline variability through time with climatic change, coupled with modern environmental sulfur contamination, also renders the production of the isoscapes necessary for the spatial assignment of sulfur isotope data in archaeological case studies difficult. Despite this, isoscapes built around archaeological data sets can provide useful approximations of anticipated geographical variability in environmental $\delta^{34}S$ values (e.g., Bataille et al., 2021). Furthermore, at any given site, it is still possible to interpret $\delta^{34}S$ values of faunal bone collagen from broadly contemporary samples within a relative framework, allowing the identification of individuals or particular taxa/groups that may deviate from the range of $\delta^{34}S$ values typically measured in fauna at that site and therefore identifying them as having inhabited a distinct area or range during life. In studies seeking to directly reconstruct seasonal movement habits or identify the use of particular areas of the landscape, however, alternative methods such as strontium isotope analysis are required.

Strontium isotope analysis The $^{87}Sr/^{86}Sr$ ratio of herbivore enamel (bioapatite) is directly related to the $^{87}Sr/^{86}Sr$ ratio of ingested plants. This, in turn, is a product of the soils and water available to the plants and ultimately correlates with underlying lithologies, with the relative content of ^{87}Sr to ^{86}Sr being a function of the age of the rock as well as its mineral composition and original chemical content (Capo et al., 1998; Bentley 2006). Generally, higher $^{87}Sr/^{86}Sr$ values are demonstrated in older rocks, and lower values in younger rocks. When combined with serial sampling, the strontium isotope analysis of incrementally growing tissues (e.g., tooth enamel) can permit the reconstruction of seasonal movements. A small number of archaeological studies have used these methods to explore the spatial paleoecology and migratory behavior of Late Pleistocene fauna, including members of the extinct genus *Mammut* (e.g., Hoppe et al., 1999; Wooller et al., 2021) and Late Pleistocene European *Rangifer* (e.g., Britton et al., 2011; Price et al., 2017). Significantly, the use of modern materials has allowed an assessment of the relationship between movement histories and the isotopic values exhibited in *Rangifer* enamel—confirming the relationship between environmental and geological conditions, known movements, and dental isotope chemistry (Britton et al., 2009; Britton 2010).

There are, however, several caveats and considerations related to the use of strontium isotope analysis in inferring animal movements. The careful selection of samples is imperative, requiring teeth that form over a period sufficient to capture at least a year of isotopic inputs. This may, in some cases, mean multiple teeth are required from the same animals, for example, in *Rangifer* (Britton et al., 2009). Data are typically then obtained via the sequential sampling of enamel as horizontal bands down the crown followed by ion-exchange column chemistry to isolate the strontium in the sample, before mass spectrometry (e.g., Britton et al., 2011; Funck et al., 2020), or via the direct laser ablation of the enamel (e.g., Wooller et al., 2021). The selection of which technique has implications for data precision, sample destruction, and the resolution achievable (see discussion in Boethius et al., 2022 for a recent summary), but studies of modern animals of known movements have established both techniques as an effective means of reconstructing movements during the period of tooth formation (e.g., wild migratory *Rangifer*, Britton et al., 2009; domestic sheep, Lazzerini et al., 2021). The analysis of different individuals from the same herd in both these modern cases has also allowed an assessment of the expected level of intraherd variability.

Finally, to interpret intratooth strontium data and assess mobility patterns, the establishment of local predicted environmental bioavailable strontium is required, ideally within the framework of a wider isoscape. The deviations between $^{87}Sr/^{86}Sr$ variability predicted purely from geological maps, and bioavailable strontium found in soils has been discussed extensively in the literature (see reviews in Capo et al., 1998; Bentley 2006; Britton 2020). Instead of relying on geological maps, isoscapes of bioavailable strontium are typically developed through the determination of $^{87}Sr/^{86}Sr$ in modern rock or soil leachates, local waters, plant, or faunal samples to generate source data, with the selection of analyte potentially influencing the isoscape produced (see discussion in Britton et al., 2020). These source data are then combined to produce spatial maps of strontium isotopic variation across landscapes using a variety of GIS-based or spatial aggregation techniques (see review in Holt et al., 2021). The inference of movement can then be made through visual comparison of variation in data with variation within those isoscapes, or with the assistance of spatial assignment software tools (e.g., Ma et al., 2020).

Oxygen isotope analysis There are several different applications for oxygen isotope analysis in zooarchaeology and paleoecology, all based on the relationship between the oxygen isotope composition ($\delta^{18}O$) of an animal's body tissues and that of water consumed (Longinelli, 1984; Luz et al., 1984; Iacumin et al., 1996; Kohn, 1996). The oxygen isotope composition of environmental water is closely related to the $\delta^{18}O$ values of precipitation, reflecting local temperatures and other factors (Dansgaard, 1964; Yurtsever, 1975; Gat, 1980; Clark and Fritz, 1997). Although hydrological processes such as water movement, water mixing, groundwater recharge, and the formation (and evaporation) of surface water bodies can all influence the oxygen isotope composition of local environmental water (and, by inference, drinking water), broad correlations between groundwater, mean annual precipitation, and climate at specific locales are universally apparent (see review in Pederzani and Britton, 2019). In obligate drinking mammals, where local environmental waters are the primary source of fluids imbibed, the relationship between the $\delta^{18}O$ values of local environmental water and the $\delta^{18}O$ values of an animal's body tissues is mediated by the $\delta^{18}O$ values of body water. Homeothermic mammals have a metabolically controlled, relatively constant body temperature (~37 °C), and therefore the bioapatite (a carbonated hydroxyapatite) in their mineralized tissues precipitates in oxygen isotope equilibrium with body water at this temperature (Longinelli, 1984; Luz et al., 1984; Levinson et al., 1987). There is, therefore, a roughly linear relationship between the $\delta^{18}O$ values of ingested water, body water, and bioapatite, and this relationship has led to the application of $\delta^{18}O$ to archaeological and paleontological remains as a means of reconstructing past climatic conditions. Although some variation in this relationship has been noted between species, fractionation factors have been established for several different taxa based on modern experimental studies (e.g., Delgado Huertas et al., 1995

[horses]), allowing the development of these techniques on faunal remains from archaeological sites as a means of reconstructing past paleotemperatures.

Paleothermic reconstructions using the oxygen isotope analysis of faunal remains from European Late Pleistocene sites have focused on a range of different mammalian species and have used analyses of both the carbonate (CO_3) and phosphate (PO_4) components of tooth enamel (e.g., Delgado Huertas et al., 1997; Fabre et al., 2011; Skrzypek et al., 2011; Kovács et al., 2012). As obligate drinkers with significant daily water requirements, and taxa found in both glacial and interglacial faunal assemblages, equids and large bovids are particularly useful for mapping past $\delta^{18}O$ precipitation values and paleoclimate conditions. The analyses of these taxa from anthropogenically derived (archaeofaunal) assemblages have the potential to generate terrestrial paleoclimate proxy data near-synchronous to human site-use, enabling estimates of mean annual temperatures when dental tissues are bulk sampled (e.g., Britton et al., 2019) and of seasonal paleotemperatures when hypsodont teeth are incrementally sampled (e.g., Pederzani et al., 2021).

In addition to the in-built assumptions inherent in the reconstruction of paleotemperatures detailed earlier, several other factors can influence data produced and thus paleotemperature estimates. For example, the choice of tooth sampled is important. Early forming teeth, in general, should be avoided because of a known enrichment in ^{18}O in the body water (and thus tissues) of juvenile animals during nursing compared to adult individuals (see review in Pederzani and Britton, 2019). Sampling strategy therefore must incorporate knowledge of likely age-at-weaning for species targeted. As well as tooth selected, method of sampling can influence data generated (Reade et al., 2015). In the determination of bioapatite $\delta^{18}O$ values, different moieties can be targeted, influencing data obtained. In paleotemperature reconstructions using older Paleolithic materials, phosphate is often the favored analyte as it is generally considered to be more resistant to postdepositional alteration compared to the carbonate component (Iacumin et al., 1996; Zazzo et al., 2004). Furthermore, the vast majority of modern calibration data for converting bioapatite $\delta^{18}O$ values to predicted $\delta^{18}O$ drinking water values has so far been generated from phosphate data and the use of carbonate $\delta^{18}O$ values ($\delta^{18}O_{CO_3}$) for paleotemperature estimation would therefore require an additional conversion step to predicted $\delta^{18}O$ values of bioapatite phosphate ($\delta^{18}O_{PO_4}$) before paleotemperature calculations, which can increase uncertainty. Conversion equations themselves, which are required to convert $\delta^{18}O_{PO_4}$ to estimates of the $\delta^{18}O$ values of drinking water ($\delta^{18}O_{dw}$) and then to estimates of temperature, also include inherent assumptions and introduce (often large) compound uncertainties (Pryor et al., 2014). These conversions, and the uncertainties introduced, are discussed at length in several articles (e.g., Pryor et al., 2014; Pederzani et al., 2021).

1.3. The site of Abri du Maras

The site of Abri du Maras is located on the west bank of the Rhône River, in a small valley at the confluence of the Ardèche River (Fig. 1). The site is all that remains of a vast southeast-facing rock shelter, situated today 70 m above the river itself at the outer edge of the gorge. The Rhône Valley lies between mountainous regions—the Massif Central to the west and the foothills of the Alps to the east—with the valley itself connecting more northerly parts of France to the Mediterranean. Many tributaries, including the Ardèche River, connect the Rhône River to the Massif Central. Archaeological and zooarchaeological evidence from the region's caves and rock shelters suggest a farsighted circulating subsistence model closely associated with the regional microtopography, interactions with nonhuman carnivores and the estimated availability of (seasonal) resources including prey-species, biotopes, and raw material outcrops (Daujeard and Moncel, 2010; Daujeard et al., 2016). Monospecific prey assemblages, characterized by the high dominance of remains of a single species represented by a large (minimum) number of individuals (Gaudzinski, 2006), are found at some Middle Paleolithic sites in the region, including at Abri du Maras with *Rangifer* (Daujeard and Moncel, 2010; Moncel and Daujeard, 2012; Daujeard et al., 2012, 2019; Marín et al., 2020; Moncel et al., 2021). Monospecific faunal assemblages increase significantly all over Europe from MIS 5 onwards, and when involving animals that live in large herds, such as reindeer, are often linked to cooperative and planned mass hunting strategies, and flexible resource utilization against a background of increasing climatic instability (Gaudzinski, 2006). In such contexts, understanding the spatial paleoecology of the prey taxa can be key to interpreting these human hunting practices (e.g., interception hunting; Britton et al., 2011).

Since 2009, excavations of the site have focused on Middle Paleolithic deposits, including stratigraphic unit 5 (bottom of the currently documented sequence at the site, dating to the end of MIS 5) and overlying unit 4, which contains two archaeological levels in its upper part (levels 4.1 and 4.2), which both date to MIS 3. The site has been dated by electron spin resonance and Uranium—Thorium (U—Th) methods, with level 4.1 dating to between 46 ± 3 ka and 40 ± 3 ka and level 4.2 yielding dates ranging between 55 ± 2 and 42 ± 3 ka (Richard et al., 2015). Further analyses of two enamel hydroxyapatite samples from level 4.2 using these same methods have yielded ages of 42 ± 3 and 42 ± 6, which together with an infrared stimulated luminescence age of 46 ± 4 ka confirm the attribution of this site to MIS 3 (Richard et al., 2021). Both levels contain the well-preserved evidence of hominin occupation, including abundant lithic artifacts, rare cordage remains, traces of combustion and diffuse ash lenses, and anthropogenically modified faunal remains. The lithic assemblage comprises Levallois products and other core technologies, and includes retouched flakes, blades projectile tips, and points largely made of local and semilocal flint (Hardy et al., 2013, 2020; Moncel et al., 2014; Daujeard et al., 2019; Ruebens et al., 2022). Despite being close in date (or even subcontemporaneous), levels 4.1 and 4.2 have yielded very different faunal and seasonality-indicator data, along with slightly different patterns of butchery which may suggest site use by two distinct groups with contrasting traditions (Vettese et al., 2022). The faunal spectrum in 4.2 is varied and comprises, in order of abundance, *Rangifer tarandus*, *Equus ferus* cf. *germanicus*, *Bison priscus*, *Cervus elaphus*, and *Megaloceros giganteus*, with spring-summer and autumn human occupations. Level 4.1 is largely dominated by *Rangifer* which, combined with indicators of selective butchery and autumn season of death mortality profile, is suggestive of seasonally restricted, cooperative and planned mass *Rangifer* hunting strategy and short-term occupations (Daujeard et al., 2019; Moncel et al., 2021; Vignes, 2021; Supplementary Online Material [SOM] Table S1). Understanding potential differences in the paleoecology of species exploited, particularly the spatial ecology of *Rangifer*, would be an important step in better understanding Neanderthal subsistence strategies in these different levels.

Aside from the (macro-) faunal remains, paleoenvironmental studies have been limited for levels 4.1 and 4.2 of the site. Micromammals are scarce, largely due to poor preservation, although the presence of a single sample of *Microtus* ex gr. *arvalis-agrestis* found in level 4.1 is consistent with a rather open environment (Daujeard et al., 2019). Dental microwear analysis of reindeer from level 4.1 has indicated grass-dominated mixed feeding, which is also consistent with an open environment, complementing the results of a small isotopic pilot study on faunal material from the same level indicating a lack of dense forest cover (Daujeard et al., 2019).

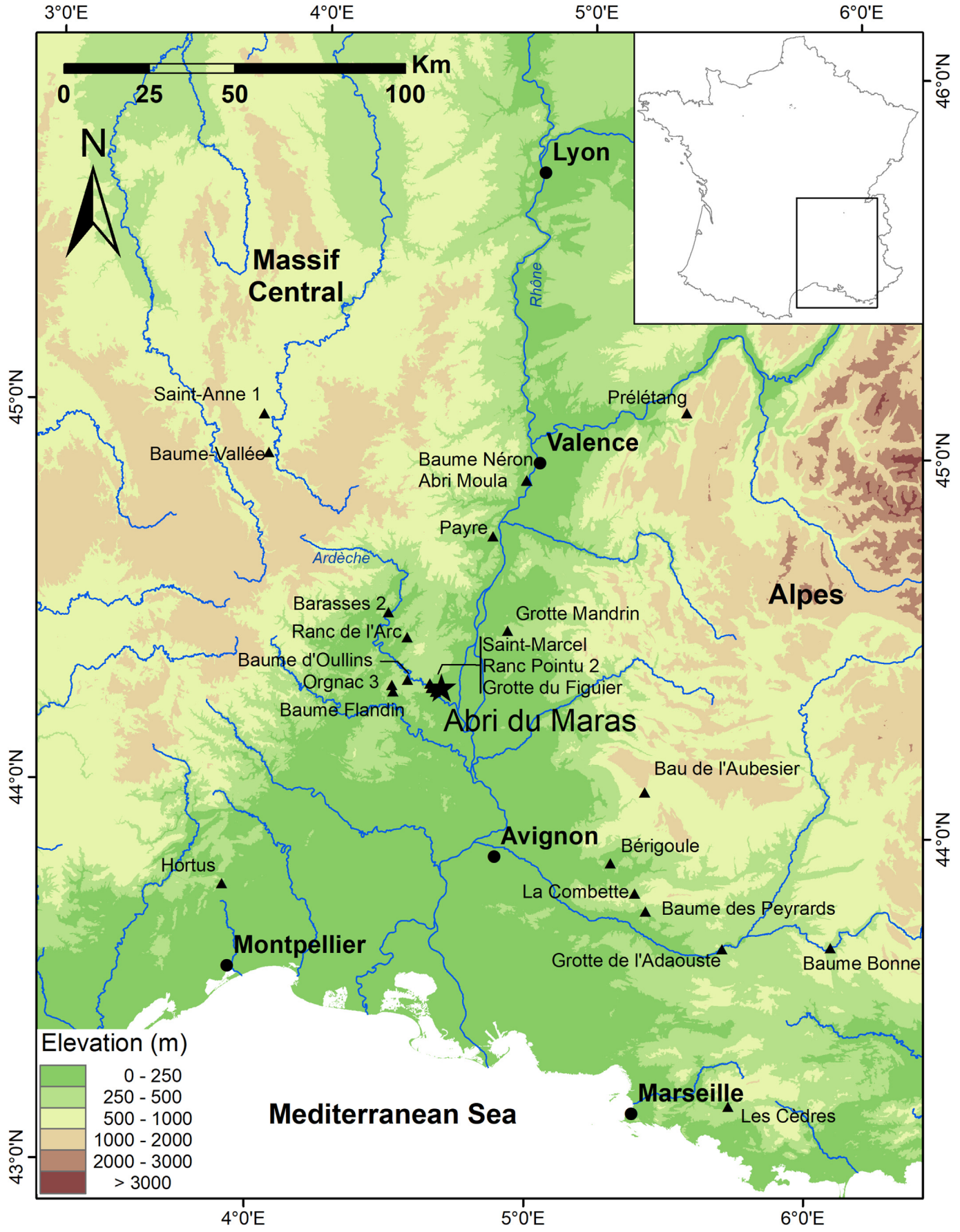

Figure 1. Elevation map of the Rhône Valley (southeast France) showing the location of Abri du Maras and other key Middle Paleolithic sites in the region.

Charcoal identified in both levels 4.1 and 4.2, however, suggest the presence of at least some woodland and taxonomic analyses has identified *Pinus sylvestris* type in both levels 4.1 and 4.2, along with *Betula* in level 4.1 only (Daujeard et al., 2019). While *P. sylvestris* grow in dry and cold conditions, *Betula* require higher soil humidity rates, which may indicate that, in level 4.1 at least, conditions may have been relatively humid/milder (which is in agreement with the results of sedimentological analysis for the site, see Daujeard et al., 2019; Moncel et al., 2021). These data may seem somewhat contradictory to the presence of *Rangifer*, which are often considered a cold-adapted species and therefore inferring a harsh or steppic environment. However, it should be noted that there are multiple ecotypes of *Rangifer* today (Festa-Bianchet et al., 2011) and the behaviors and habitat preferences of Late Pleistocene European *Rangifer* (and variation therein) should not be assumed. Furthermore, it has long been recognized that the environments of northern Europe during MIS 3 (and at other phases of the Late Pleistocene) were nonanalogous to any modern environment, that is, characterized by combinations of animals (and plants) living together that are not found in sympatry today (see Stewart, 2005 for discussion of Europe as a whole, and Foury et al., 2016 for discussion of the Rhône Valley specifically). Therefore, given the limited paleoenvironmental data available from Abri du Maras, the diversity of species present (i.e., *Rangifer* with two other cervids, including the extinct *Megaloceros*) at the site, and the differences in prey selection and seasonality of site use indicated from past zooarchaeological studies between levels 4.1 and 4.2, elucidating further information about the paleoecology of the species exploited, or the broader paleoenvironmental suite, using isotope zooarchaeological approaches is of key interest.

Here, we present the results of a multi-isotope, multitissue study of herbivore remains from level 4.1 (46 ± 3 to 40 ± 3 ka) and level 4.2 (55 ± 2 to 42 ± 3 ka) at the Middle Paleolithic site of Abri du Maras (Ardèche, France), with the goal of providing new insights into the paleoenvironmental and paleoecological context of Neanderthal activity in the Rhône Valley during MIS 3. The specific aims of this study are as follows: (1) to provide evidence of local paleothermic conditions; (2) to assess niche feeding behaviors and landscape use by key subsistence species; and (3) to examine potential relationships between herbivore ecology and/or seasonal biogeography at the site, the paleoenvironment, and the subsistence behaviors of contemporary hominin groups.

2. Materials and methods

2.1. Sample selection

Ungulate bone and teeth from the recent excavations at Abri du Maras (levels 4.1 and 4.2) were selected for destructive sampling and isotope analysis, including teeth of *Equus* and *Rangifer* for oxygen and strontium isotope analysis, respectively, and *Bison*, *Cervus*, *Equus*, *Megaloceros*, and *Rangifer* bone for carbon, nitrogen, and sulfur isotope analysis (see Table 1 for all samples involved in this study). These samples are part of collections currently housed at the Institut de Paléontologie Humaine (IPH), Paris, for their ongoing study following taxonomic identification.

Owing to sample availability, two complete *Equus* mandibular second premolars were sampled and analyzed for oxygen ($\delta^{18}O$) isotope analyses for climate reconstruction from level 4.2 only. Depending on the extent of tooth wear, horse second premolar

Table 1
Faunal specimens from Abri du Maras used in this study, including unique site sample identifier (corresponding to excavation square and find number), stratigraphic level, component sampled, and analyses undertaken.[a]

Site sample ID (Square-Number)	Level	Species	Component sampled	Isotopic data obtained				
				$\delta^{13}C$	$\delta^{15}N$	$\delta^{34}S$	$^{87}Sr/^{86}Sr$ (sequential)	$\delta^{18}O$ (sequential)
*L6-54	4.1	*Equus*	Metacarpal 3	x	x	x		
*J6-29	4.1	*Equus*	Mandible	x	x	x		
*G6-86	4.1	*Equus*	Mandible	x	x	x		
L6- 10008	4.1	*Equus*	LM_3				x	
*H7-70	4.1	*Megaloceros*	Mandible	x	x	x		
*H7-84	4.1	*Megaloceros*	Maxilla	x	x	x		
*M6-599	4.1	*Rangifer*	Mandible	x	x	x		
*M6-671	4.1	*Rangifer*	Mandible	x	x	x		
*M6-520	4.1	*Rangifer*	Mandible	x	x	x		
I7-133	4.1	*Rangifer*	RM_2 (pair with I7-80)				x	
I7-80	4.1	*Rangifer*	RM_3 (pair with I7-133)				x	
J6-306	4.1	*Rangifer*	LM_2, LM_3				x	
N6-178	4.1	*Rangifer*	LM_2, LM_3				x	
N6-687	4.2	*Equus*	LP_2					x
N6-767	4.2	*Equus*	RP_2					x
L11-17	4.2	*Bos/Bison*	Mandible	x	x	x		
L11-27	4.2	*Bos/Bison*	Crania	x	x	x		
M6-948	4.2	*Cervus elaphus*	Mandible	x	x	x		
N6-872	4.2	*Cervus elaphus*	Mandible	x	x	x		
L7-328	4.2	*Cervus elaphus*	Mandible	x	x	x		
G8-44	4.2	*Cervus elaphus*	Mandible	x	x	x		
K7-196	4.2	*Cervus elaphus*	Mandible	x	x			
J6-536	4.2	*Equus*	Mandible	x	x			
L7-286	4.2	*Equus*	Mandible	x	x	x		
M10-17	4.2	*Equus*	Mandible	x	x	x		
L6-769	4.2	*Equus*	Mandible	x	x			
L11-26	4.2	*Equus*	Mandible	x	x	x		
L7-335	4.2	*Megaloceros*	Maxilla	x	x			
L7-307	4.2	*Megaloceros*	Maxilla	x	x	x		
M10-121	4.2	*Rangifer*	Mandible, LM_2, LM_3	x	x		x	

Abbreviations: Site sample ID = unique identification label assigned on site, corresponding to square and find number; L = left; R = right.
[a] Mean carbon and nitrogen isotope data from initial analyses of some samples (indicated by an asterisk) were first published in Daujeard et al. (2019). Please note mean values presented in that article do not incorporate the new analyses undertaken here.

enamel mineralizes between the ages of ~13 and 31 months, allowing the inference of more than a year of isotopic inputs (Hoppe et al., 2004). Weaning in horses generally takes place before the start of second premolar development, meaning that any nursing effects on $\delta^{18}O$ values are avoided by choosing this tooth type (Hoppe et al., 2004). A third *Equus* tooth, a third molar, suitable for analyses was recovered from level 4.1, but was only analyzed for $^{87}Sr/^{86}Sr$ (see below, section 2.5) but not $\delta^{18}O$. As different tooth positions exhibit different enamel mineralization rates throughout tooth growth, they are not exactly comparable in their seasonal $\delta^{18}O$ values patterns, a concern particularly in horses (Bendrey et al., 2015). As this M3 was the only available *Equus* tooth specimen from level 4.1 any interlevel difference in $\delta^{18}O$ values could not be securely assigned to environmental differences but could also be an artifact from comparing different tooth positions. For this reason, we decided not to sample this tooth for $\delta^{18}O$. No bone was sampled from these individuals because of them being loose teeth.

To explore the seasonal mobility of *Rangifer*, two mandibular teeth (second and third molars) were selected from four *Rangifer* for strontium ($^{87}Sr/^{86}Sr$) isotope analyses. Owing to the availability of material, samples included three individuals from level 4.1, but only a single individual from level 4.2. Although intratooth $\delta^{18}O$ values can be helpful in 'anchoring' $^{87}Sr/^{86}Sr$ within a seasonal context, given that *Rangifer* are nonobligate drinkers and long-distance and/or altitudinal migrations can cause intratooth $\delta^{18}O$ profiles to deviate substantially from a classic seasonal sinusoid (Britton et al., 2009), coupled with the need for minimally destructive intratooth sampling, the decision was made not to sample the *Rangifer* teeth for oxygen isotope analysis. However, in the absence of oxygen isotope data, the periodicity of *Rangifer* tooth crown formation and mineralization, and thus the seasonality of intratooth $^{87}Sr/^{86}Sr$ can still be approximated based on previous studies, including a single radiograph study (Wu et al., 2012) and from comparable data sets from other cervid species. For example, Brown and Chapman (1991: 373) determined that formation of the second and third molar crowns of *Dama dama* commence at <3.5 and 9 months of age and complete at 9 and <18 months, respectively. Although intratooth oxygen isotope studies on *Rangifer* are not straightforward for the reasons stated earlier, the scant intratooth oxygen isotope data from modern migratory and nonmigratory individuals (Britton et al., 2009; Britton 2010) suggest these estimates of enamel mineralization time are appropriate. Therefore, sampling of these second and third molars can (depending on the extent of wear) provide evidence of calving grounds, summer and winter range during the first year of life, and summer/autumn range during the second year of life (Britton et al., 2009). It must be noted, however, that any intratooth isotope study using archaeological materials has unavoidable assumptions inbuilt with regard to both the growth rate/mineralization time and birth seasonality of ancestral species being similar to extant individuals today. Anticipated to be a likely nonmigratory species, an *Equus* third molar was selected from level 4.1 for strontium isotope analyses as a comparator to the *Rangifer*.

Following on from a previous pilot study of stable carbon ($\delta^{13}C$) and nitrogen ($\delta^{15}N$) isotopic niche variability in *Equus* ($n = 3$), *Megaloceros* ($n = 2$), and *Rangifer* ($n = 3$) from level 4.1 (Daujeard et al., 2019), further bone samples from five ungulate taxa were selected for collagen extraction and analyses from level 4.2, including *Equus* ($n = 5$), *Megaloceros* ($n = 2$), *Rangifer* ($n = 1$), *Bison* ($n = 2$), and *C. elaphus* ($n = 5$). It should be noted that, with the exception of the *Rangifer* sample from level 4.2 (M10-121) from which both mandibular teeth and bone were sampled, bone samples and the teeth sampled for strontium and oxygen described did not (to our knowledge) originate from the same individuals. Although, ideally, these different isotope analyses would be undertaken from the same individuals, the horse teeth were all loose and it was not possible to sample the mandibles from the reindeer from which teeth were selected in level 4.1 because of their poor preservation/friability. Conversely, although bone was successfully sampled from other *Rangifer* mandibles in level 4.1, their teeth were insufficient for strontium isotope analyses (e.g., lacking in a complete and relatively unworn second and/or third molar, both of which are required to reconstruct a full year of movement history).

2.2. Tooth and bone sampling protocols

For all teeth, the buccal face of the anterior loph was selected for sampling as it tends to have thicker enamel than the lingual side. The whole face was abraded (using air abrasion) to remove superficial enamel. Each complete tooth was then ultrasonicated in Milli-Q ultrapure water for 5 min. Incremental enamel samples were taken as horizontal bands, perpendicular to the tooth growth axis, using a diamond-coated tungsten carbide cutter point (NTI-Kahla) from the enamel–root junction (ERJ) to the occlusal surface. Sampling increments were 1–2 mm, measured as distances from the ERJ in each specimen using digital calipers. For the *Equus* from level 4.2, between 25 and 28 samples of fine enamel powder, ranging in weight from ~5 to ~15 mg, were collected from each tooth. For the *Rangifer*, between 5 and 10 serial samples of fine enamel powder, ranging in weight between ~3 and ~8 mg (albeit with a single sample, SEVA32976IX, weighing ~1 mg) were collected from each tooth depending on crown height available to sample/extend of wear. A single sample of dentine, presumed to be diagenetically altered and therefore reflecting of local soil values, was taken from the molar roots of each of the *Rangifer* teeth sampled in order to provide a secondary indicator of local environmental $^{87}Sr/^{86}Sr$ at the site. For the single *Equus* tooth from level 4.1, three samples, spaced evenly down the crown (~12–14 mm apart), were taken in a similar way. Bone (~1–2 g) was sampled for collagen extraction using rotary stainless-steel cutting implements and cleaned using air abrasion.

2.3. Oxygen isotope analysis

Silver phosphate precipitations and mass spectrometry Serial samples of *Equus* tooth enamel (~10 mg) were prepared for phosphate oxygen isotope analysis in the Archaeological Chemistry Laboratories, Department of Archaeology, University of Aberdeen following methods described in Britton et al. (2019) using a rapid precipitation method, after Tütken et al. (2006) and based on O'Neil et al. (1994) and Dettmann et al. (2001: Appendix, GSA Data Repository item 20018), with minor modifications.

Phosphate $\delta^{18}O$ values were determined by continuous flow isotope ratio mass spectrometry (CF-IRMS), measured with a Thermo-Fisher thermal conversion elemental analyzer (TC-EA) connected to a Finnigan Delta Plus XL mass spectrometer, at the Department of Geochemistry, University of Tübingen, Germany. Mean values and standard deviations (1 SD) were provided by the analyzing laboratory, calculated from the analysis of each sample in triplicate (SOM Table S2). In some instances, mean values were provided from duplicate measurements, due to small sample size, sample loss, loss of sample integrity, or through internal data quality control checks in Tübingen (SOM Table S2). Long-term laboratory reproducibility was reported as ±0.3‰ (1 SD), whereas mean reproducibility for the samples analyzed in this study was ±0.2‰ (1 SD) or better. A detailed description of silver phosphate precipitation and the calibration of mass spectrometry data and standards can be found in SOM S1.

Modeling of intratooth oxygen isotope data, conversion equations and air temperature estimations The extended process of tooth enamel growth and mineralization of ungulate teeth causes a predictable damping of the seasonal amplitude of oxygen isotopic change expressed tooth enamel compared to the seasonal amplitude in consumed environmental water (Kohn et al., 1996; Passey and Cerling, 2002; Kohn, 2004; Blumenthal et al., 2014; Green et al., 2017; Trayler and Kohn, 2017). Therefore, a correction procedure is necessary to obtain faithful paleotemperature reconstructions on a seasonal time scale, which can be achieved using an inverse model (Passey et al., 2005; Green et al., 2018). Such models take into account the sampling geometry and species-specific characteristics of tooth enamel formation to estimate the original $\delta^{18}O$ input. In this study, horse tooth enamel $\delta^{18}O$ seasonal curves were inverse modeled following methods in Passey et al. (2005) using R v.4.1.2 (R Core Team, 2021) and an R code translation of the originally published MATLAB code. Details of the modeling procedure are described in SOM S2 and we provide all code and data necessary to reproduce this step in the SOM File S1.

Corrected summer peak and winter trough $\delta^{18}O$ values were extracted from the most likely model solutions and used to estimate summer and winter paleotemperatures following methods in Pryor et al. (2014), and are described in more detail in SOM S2. Mean $\delta^{18}O$ values were computed as the mean of unmodeled summer peak and winter trough values, rather than as annual averages, following comparisons in Pederzani et al. (2021) showing that summer/winter means and year-long averages of modeled or unmodeled $\delta^{18}O$ sinusoidal curves yield essentially identical results. However, to indicate that these values do not represent averages of complete annual cycles, we refer to them as 'midpoints' to avoid confusion. Details of the temperature estimation procedure are provided in SOM S2, and we provide the spreadsheets that were used for all estimations in SOM File S1.

2.4. Bone collagen extraction and analysis

Collagen was extracted using the Longin (1971) method, with modifications based on the recommendations of Collins and Galley (1998), and with the addition of an ultrafiltration step (Brown et al., 1988), as described in Britton et al. (2012). Collagen samples were analyzed (in duplicate) for stable carbon ($\delta^{13}C$) and nitrogen ($\delta^{15}N$) isotope ratios at the Department of Human Evolution, Max Planck Institute for Evolutionary Anthropology (MPI-EVA, Leipzig, Germany), on a Delta XP mass spectrometer coupled to a Flash EA 2112 elemental analyzer, with an analytical precision of ±0.3‰ (1 SD) or better based on replicate analyses of an in-house methionine standard. See SOM S3 for details of data normalization and standards (in-house and international).

An additional aliquot of collagen was analyzed for stable sulfur ($\delta^{34}S$) isotopes at the Scottish Universities Research Centre (SUERC) for all remaining collagen extracts, including those from which $\delta^{13}C$ and $\delta^{15}N$ data have been previously presented (Table 1; Daujeard et al., 2019). This was conducted on a Delta V Advantage continuous-flow isotope ratio mass spectrometer coupled via a ConfloIV to an IsoLink elemental analyzer (Thermo Fisher Scientific, Bremen, Germany), a system that enables the comeasurement of carbon, nitrogen, and sulfur stable isotope ratios (Sayle et al., 2019), generating additional $\delta^{13}C$ and $\delta^{15}N$ measurements as well as $\delta^{34}S$ measurements with an analytical precision of ±0.3‰ (1 SD) or better for each isotope (see SOM S4 for method statement and details of normalization of data and standards). As multiple sets of $\delta^{13}C$ and $\delta^{15}N$ measurements were obtained from each sample (see SOM Tables S3 and S4 for MPI-EVA and SUERC data, respectively), for the purposes of this study, the calculated mean of all measurements is used for each sample (SOM Table S5), which slightly modifies the values reported for some of the same samples from level 4.1 previously reported in Daujeard et al. (2019). However, across the two laboratories, the average standard deviation (1 SD) about the mean for the measurement of all individual aliquots was lower than the largest long-term reproducibility/analytical error reported by either laboratory. Thus, the data are considered comparable. No subsequent statistical treatments were applied to the carbon and nitrogen isotope data, beyond the descriptive statistics in the text below (mean, standard deviation, etc.). However, we explored the partition of the samples according to their $\delta^{34}S$ values using hierarchical clustering ('hclust' base function, R v.4.1.2). We used the 'average' agglomeration method to define the clusters as it provided the highest cophenetic correlation coefficient for our data set ($c = 0.896$) among the different agglomeration methods (Legendre and Legendre, 1998).

2.5. Strontium isotope analysis

Sample preparation and mass spectrometry All samples of *Rangifer* tooth enamel (plus the dentine, and three sub-samples of *Equus* tooth enamel from level 4.1) were analyzed for strontium isotope ratios using the ion-exchange solution method described in Copeland et al. (2008) and Britton et al. (2009), a modification of the method from Deniel and Pin (2001). $^{87}Sr/^{86}Sr$ ratios were determined using a Thermo Fisher (Thermo Fisher Scientific) Neptune multicollector inductively coupled plasma mass spectrometer (MC-ICP-MS) in the Department of Human Evolution at the Max Planck Institute for Evolutionary Anthropology. Strontium concentrations of the enamel samples were determined using the method described in Copeland et al. (2008), which is accurate to within ±31 ppm. Analytical precision was ±0.00003 (2 SD) or better, based on the repeat analysis of external and in-house standards. For detailed descriptions of sample preparation, correction of mass spectrometry data, and details of standards and blanks, see SOM S5.

Spatial assignment For the four *Rangifer*, in addition to the generation of individual intratooth profiles (see section Results below), and one *Equus*, spatial assignment of strontium isotope data from three points during tooth growth in each individual tooth-pair was undertaken using the 'assignR' package v.2.2.0 in R (Ma et al., 2020). Assignment of the *Equus* samples were done as a reference for a (presumably) local, nonmigratory species. The 'assignR' package permits the inference of geographical origin from isotope data, with assignments in the case of $^{87}Sr/^{86}Sr$ based on variability of environmental $^{87}Sr/^{86}Sr$ across the landscape (the strontium isoscape; Fig. 2). We used the global bioavailable $^{87}Sr/^{86}Sr$ isoscape, and the associated spatial error raster produced by Bataille et al. (2020). The three sample locations in each *Rangifer* sampled selected for spatial assignment include the following: (1) the sample closest to the occlusal surface of the second molar (the earliest forming section of the intratooth profiles obtained, expected to broadly correspond with location during the first summer of life); (2) the sample closest to the ERJ of the second molar (broadly corresponding to location during the first winter of life); and (3) the sample closest to the ERJ of the third molar (broadly corresponding to location during the second summer/autumn of life). For *Equus*, the three samples were taken from the M3, close to the occlusal surface, at the midpoint, and close to the ERJ. For each sample, treated as sample of unknown origin, we generated the posterior probability surface of origin rescaled to 1, then we extracted the area corresponding to 80% of the posterior probability density. R code is provided in SOM File S2.

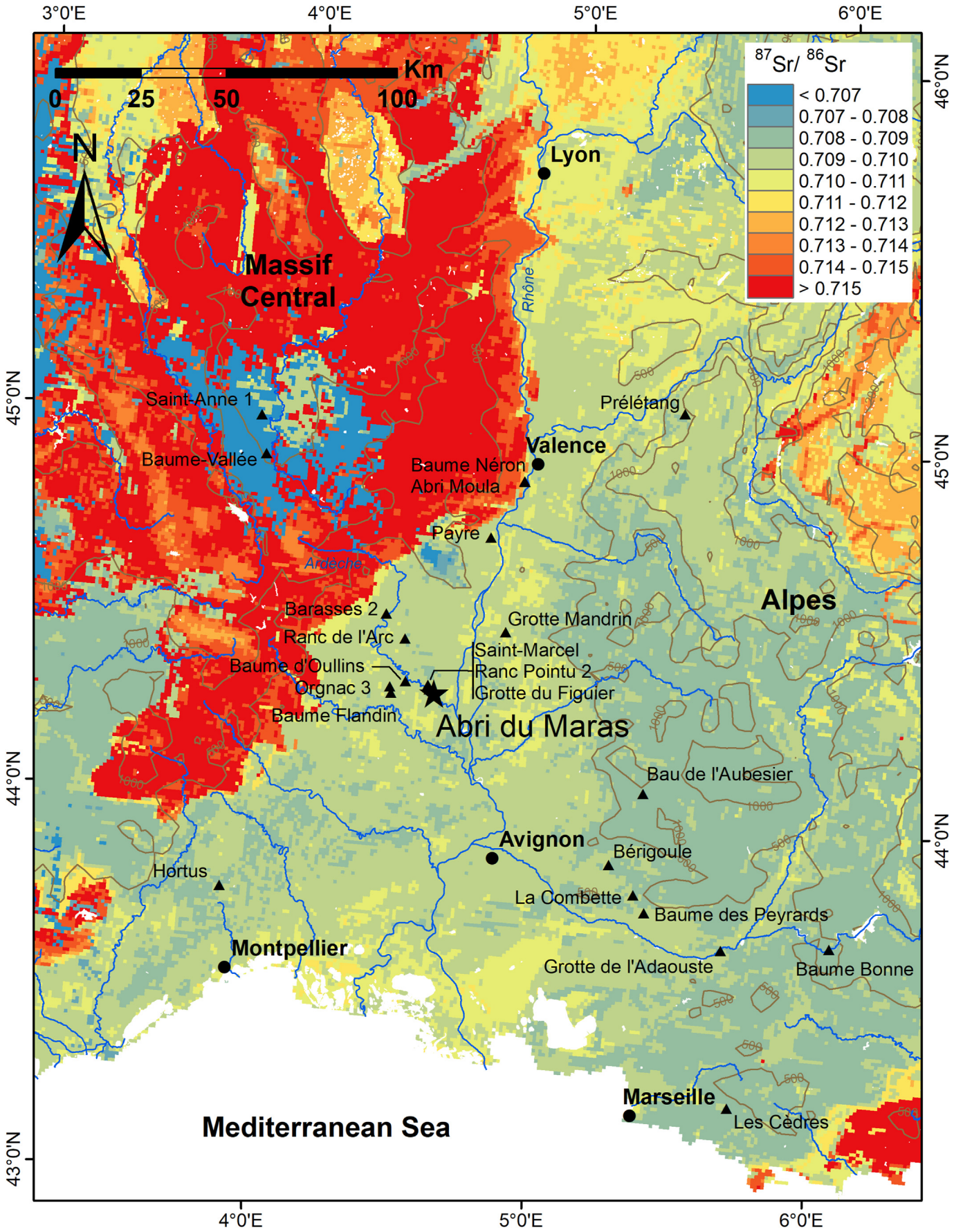

Figure 2. Strontium isoscape of the Rhône Valley (based on Bataille et al., 2020).

3. Results

3.1. Intratooth enamel oxygen isotope data from level 4.2 Equus

Oxygen isotope data generated from two *Equus* teeth (lower second premolars) from level 4.2 demonstrate sinusoidal intratooth patterns, with values ranging from 16.3 to 19.3‰ with a midpoint (mean of summer and winter extremes) of 17.8‰ (N6-767) and 15.2 to 18.9‰ with a midpoint of 17.1‰ (N6-687; Fig. 3; full data in SOM Table S2 and summary of seasonal extrema in SOM Table S6). This results in a seasonal $\delta^{18}O$ amplitude of ~3‰. Given the well-documented linear relationship between *Equus* sp. enamel $\delta^{18}O$ values and drinking water $\delta^{18}O$ values (Bryant et al., 1994; Sánchez Chillón et al., 1994; Delgado Huertas et al., 1995), we take the characteristic sinusoidal $\delta^{18}O$ curves seen here in sequentially sampled tooth enamel to be reflective of seasonal changes in $\delta^{18}O$ values of environmental water consumed by these individuals, that most likely in turn reflect seasonal temperature changes. Based on the linear relationship between $\delta^{18}O$ of enamel ($\delta^{18}O_{enamel}$) and $\delta^{18}O$ of drinking water ($\delta^{18}O_{dw}$) and in turn with $\delta^{18}O$ of precipitation, we estimated $\delta^{18}O_{dw}$ and paleotemperatures to facilitate comparisons with other paleoclimate information and with modern climates (see SOM S3 for more information). This approach relies on some inherent assumptions including a certain degree of physiological similarity between modern and Pleistocene animals, a broadly comparable system of atmospheric circulation, and that drinking water sources of the studied animals isotopically reflect precipitation inputs. These are mostly thought to be justified for European Late Pleistocene settings, although local hydrotopography and drinking water sources need to be studied on a case-by-case basis. In addition, it should be noted that they introduce a certain unavoidable (and mathematically not fully captured) degree of uncertainty to paleotemperature estimations (see Pryor et al., 2014 and SOM S2 for details on error sources that are accounted for).

An overview of unmodelled summer, mean and winter $\delta^{18}O_{enamel}$, inverse-modeled summer and winter $\delta^{18}O$, and corresponding $\delta^{18}O_{dw}$ and paleotemperature estimates is provided in SOM Table S6. Drinking water $\delta^{18}O$ estimates fall at -0.6 ± 2.1‰ for summer, -7.6 ± 2.1‰ for annual means, and -16.2 ± 2.2‰ for winter (Fig. 4). In comparison, interpolated estimates of modern precipitation $\delta^{18}O$ indicate that current precipitation at the site exhibits $\delta^{18}O$ values of -1.5‰ in July and -9.9‰ in January and mean annual $\delta^{18}O$ of -6.3 ± 0.1‰ (95% CI; Bowen and Revenaugh, 2003; Bowen et al., 2005; Bowen, 2022), Paleotemperature conversions for the two individuals from level 4.2 indicate summer temperatures of 31 ± 4.8 °C, winter temperatures of -10 ± 4.3 °C, and mean annual temperatures of 12 ± 4.0 °C (Fig. 4), where error ranges indicate the compound error of the paleotemperature estimation as described in Pryor et al. (2014). This compares to modern-day (1981–2009) temperatures of 4.3 ± 1.6 °C in January, 23.3 ± 1.1 °C in July, and an annual average of 13.4 ± 0.5 °C estimated for the site using the ClimateEU model (Marchi et al., 2020).

3.2. Bone collagen carbon, nitrogen, and sulfur isotope data of ungulates from levels 4.1 and 4.2

Full results of the faunal bone collagen extracted and analyzed from Abri du Maras can be found in the SOM (SOM Table S3 [Leipzig], SOM Table S4 [SUERC], and SOM Table S5 [means]), including all quality (%C,%N, %S, C:N, C:S, and N:S) data. $\delta^{13}C$ and $\delta^{15}N$ values of all specimens are shown in Figure 5, and corresponding $\delta^{34}S$ data of all samples with sufficient remaining collagen for that analysis are shown in Figure 6. Although approximately half of the samples have %C and %N marginally lower than that of modern collagen (i.e., less than ~35 ± 8.8 wt% for C, and 11–16 wt% for N; van Klinken 1999), their atomic C:N ratios are between 3.2 and 3.5, and are therefore within the expected range for well-preserved bone (DeNiro, 1985; Ambrose, 1990; van Klinken, 1999; Dobberstein et al., 2009). Furthermore, $\delta^{13}C$ and $\delta^{15}N$ values are not significantly correlated with %C or %N respectively, or with C:N ratios (see SOM Figs. S1–S4). The atomic C:S ratios range from 545 to 827 and the N:S ratios range from 157 to 250, and are therefore within the range expected for modern mammalian bone collagen (C:S = 600 ± 300 and N:S = 200 ± 100; Nehlich and Richards, 2009).

Mean $\delta^{13}C$ and $\delta^{15}N$ values (±1 SD) for horses ($n = 8$) are -20.3 ± 0.2‰ and 3.3 ± 0.8‰, and values are similar within both levels. Mean values from the *Bison* samples ($n = 2$), both level 4.2, are elevated relative to the horses being -19.7 ± 0.0‰ and 5.6 ± 0.0‰ for carbon and nitrogen, respectively. The three cervid taxa all have similar mean $\delta^{13}C$ (*Megaloceros*: -19.5 ± 0.1‰ [$n = 4$]; *Rangifer*: -19.9 ± 0.2‰ [$n = 4$]; *C. elaphus*: -19.8 ± 0.2‰ [$n = 5$]), but differ in their $\delta^{15}N$ values, with *C. elaphus* (all from level 4.2) having the lowest values (3.9 ± 0.4‰), *Megaloceros* have the most elevated values (5.5 ± 0.1‰) and *Rangifer* displaying the greatest range of values from 3.9 to 6.0‰ (mean = 4.8 ± 0.9‰).

Of the 23 bone collagen extractions, 19 yielded sufficient material for the measurement of sulfur isotope ratios. Although species $\delta^{34}S$ means (±1 SD) are similar in some species (e.g., *Megaloceros*: 5.2 ± 0.6‰ [$n = 3$]; *Bison*: 5.5 ± 0.2‰ [$n = 2$]; as well as between *Rangifer*: 3.7 ± 2.8‰ [$n = 4$] and *C. elaphus*: 3.3 ± 1.2‰ [$n = 4$]), there are notable differences between species and, in some cases, between levels. *Rangifer* and *C. elaphus* display a greater range of values than other species, including an outlier value of 0‰ in the single *Rangifer* sampled from level 4.2 (Fig. 6). Of the samples that have sulfur data, both *C. elaphus* ($n = 4$; level 4.2 only) and *Equus* ($n = 6$) have a fairly wide range of $\delta^{34}S$ values (from 2.0‰ to 4.9‰; and 2.3‰ to 6.8‰, respectively), although not as large as the range of sulfur isotope ratios shown in the *Rangifer* (which varies from 0.0‰ to 6.0‰). With the exception of the single *Rangifer* sample from level 4.2, according to the hierarchical cluster analysis, the animals at Abri du Maras fall into two broad groups with regard to sulfur: group 1) 4.8–6.8‰ and group 2) ~2–3.2‰ (SOM Fig. S5). All species analyzed are present in group 1, and *Equus*, *Rangifer*, and *Cervus* can be found in group 2, with animals from both levels found in each of the groups. A recently produced sulfur isoscape for the region (based on bone collagen data from the Mesolithic to the modern day) suggests that $\delta^{34}S$ values around Abri du Maras could be expected to range from 4 to 7‰ (SOM Fig. S6, based on data from Bataille et al., 2021). Thus, individuals from sulfur group 1 are consistent with this local range, but those in group 2 are comparatively low, and not consistent with values found within the immediate region.

3.3. Intratooth strontium isotope data from Rangifer and Equus from levels 4.1 and 4.2

Tooth enamel strontium (Sr) concentrations of archaeological *Rangifer* samples ranged from 86 to 200 ppm (SOM Table S7), which are similar to those measured in modern caribou (Britton et al., 2009) and domestic cattle (Evans et al., 2007). Strontium concentrations of *Equus* enamel were higher (~250 ppm), but also in line with values expected from archaeological herbivore teeth (Evans et al., 2007; Groot et al., 2020). Data from the M_2 and M_3 of intratooth samples of all three individual *Rangifer* sampled from level 4.1 bear similar isotope values (Fig. 7; SOM Table S7), ranging from 0.7085 to 0.7101 with a mean of 0.7089 ± 0.0003. This average is a little higher than the mean of three samples of horse tooth enamel sampled from a single horse from the same level, close to the

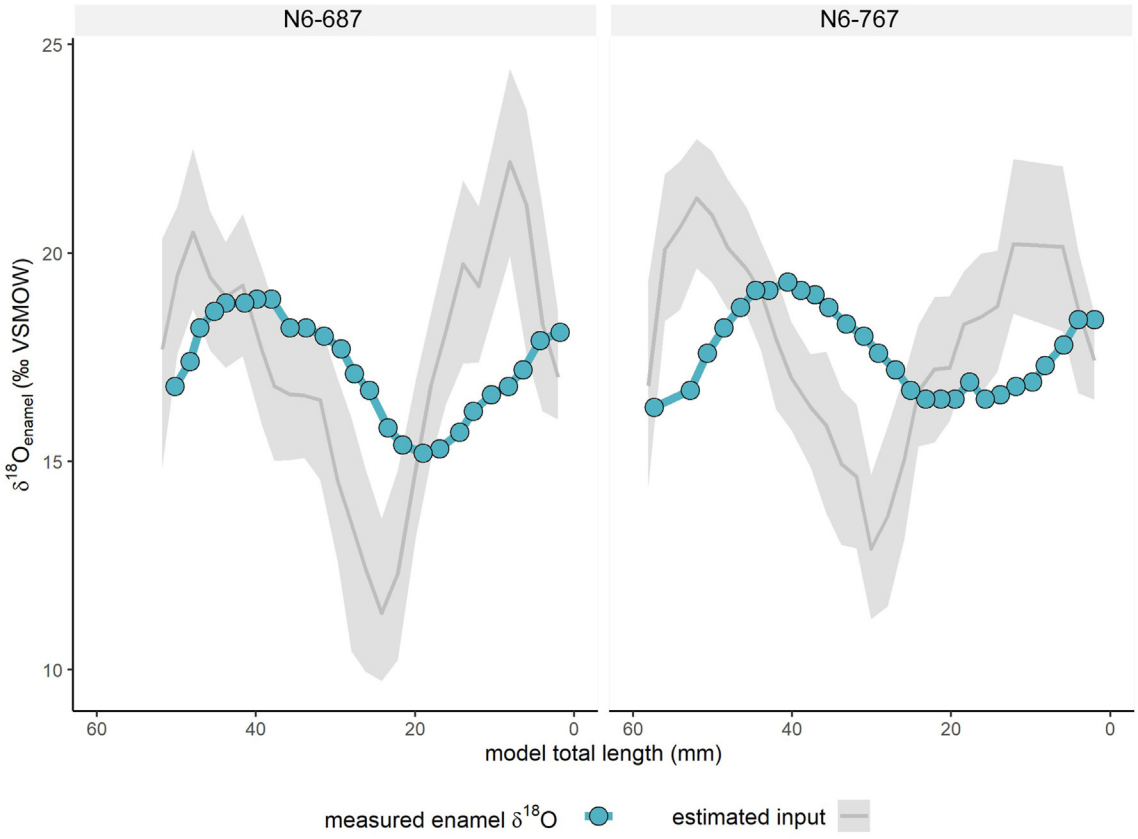

Figure 3. Measured oxygen isotope signal ($\delta^{18}O_{enamel}$; blue dots) from Abri du Maras for two *Equus* teeth (both lower second premolars, Maras 687 and Maras 767) from level 4.2, and inverse modeled isotopic input (gray line) with 95% confidence interval (gray shaded area). Abbreviation: VSMOW = Vienna standard mean ocean water. (For interpretation of the references to color in this figure legend, the reader is referred to the Web version of this article).

occlusal surface, midcrown and at the ERJ (0.7086 ± 0.0001). The strontium isotope values measured in all dentine samples from *Rangifer* from both levels 4.1 and 4.2 range from 0.7086 to 0.7092 (mean = 0.7088 ± 0.0003), are a secondary confirmation of the expected range of local values (see Fig. 2 for a predicted strontium isoscape of the region). In contrast, the intratooth values of the single reindeer individual sampled from level 4.2 show a different trend to the reindeer from level 4.1, with a higher degree of intra-tooth variability, the values ranging from 0.7090 to 0.7125 (mean = 0.7112 ± 0.0012).

The raw posterior probability distribution maps assessed from the $^{87}Sr/^{86}Sr$ spatial assignment from the three different locations on the crowns of four *Rangifer* and one *Equus* are provided in SOM Figures S7, S8, and S9. Based on the spatial assignment of the samples closest to the occlusal surface of both the M_2 and the M_3, we determined the areas where the samples have an 80% chance of originating, and considered these areas, respectively, as the winter and summer areas potentially used by each *Rangifer* (Fig. 8). For the *Equus*, we determined the potential areas corresponding to the highest and the lowest $^{87}Sr/^{86}Sr$ measurements across its intra-tooth profile, respectively, the sample closest to the M_3 ERJ (0.7086) and the sample closest to the occlusal surface (0.7085), which are almost entirely overlapping (91.8% of overlap; Fig. 8). The three *Rangifer* from level 4.1, as well as the *Equus*, show potential use of areas within of ~50 km of Abri du Maras in both winter and summer but also areas on the eastern side of the Rhône Valley or southwest of Abri du Maras (Fig. 8). Summer and winter ranges of *Rangifer* J6-306 almost overlap entirely (88.4% of overlap) and show a strong agreement with the *Equus*' range. A similar pattern is observed for *Rangifer* I7-80/I7-133 while the overlap between potential summer and winter ranges is less pronounced (48.6%). *Rangifer* N6-178 seems to show a higher segregation in its seasonal range use (21.4% of overlap) but both potential summer and winter ranges can still be found close to Abri du Maras. Spatial assignment also highlighted for this individual potential areas in summer slightly further north of Abri du Maras (Fig. 8). *Rangifer* M10-121 from level 4.2 shows a complete separation between the potential summer and winter areas (0% of overlap, Fig. 8). Summer assignment highlights areas similar to the ones used by the *Equus* and the *Rangifer* from level 4.1, in the vicinity of Abri du Maras. However, winter assignment suggests the use of areas away from Abri du Maras with potential areas located 150–200 km from the site, in the northernmost parts of the Rhône Valley or further to the east, or even more distant, in the southwest direction (Fig. 8).

4. Discussion

4.1. Paleoclimatic context

Seasonal paleotemperatures at Abri du Maras Based on the oxygen isotope data from level 4.2, and compared to modern-day temperatures at the study site (Fig. 4), the MIS 3 climate at Abri du Maras seems to have been similar, if perhaps slightly colder to modern-day conditions in terms of mean annual averages, but substantially more seasonal than today (i.e., with warmer summers, and cooler winters). It should be noted that seasonal paleotemperature reconstructions are substantially less reliable than mean annual paleotemperature estimates, because of the necessity

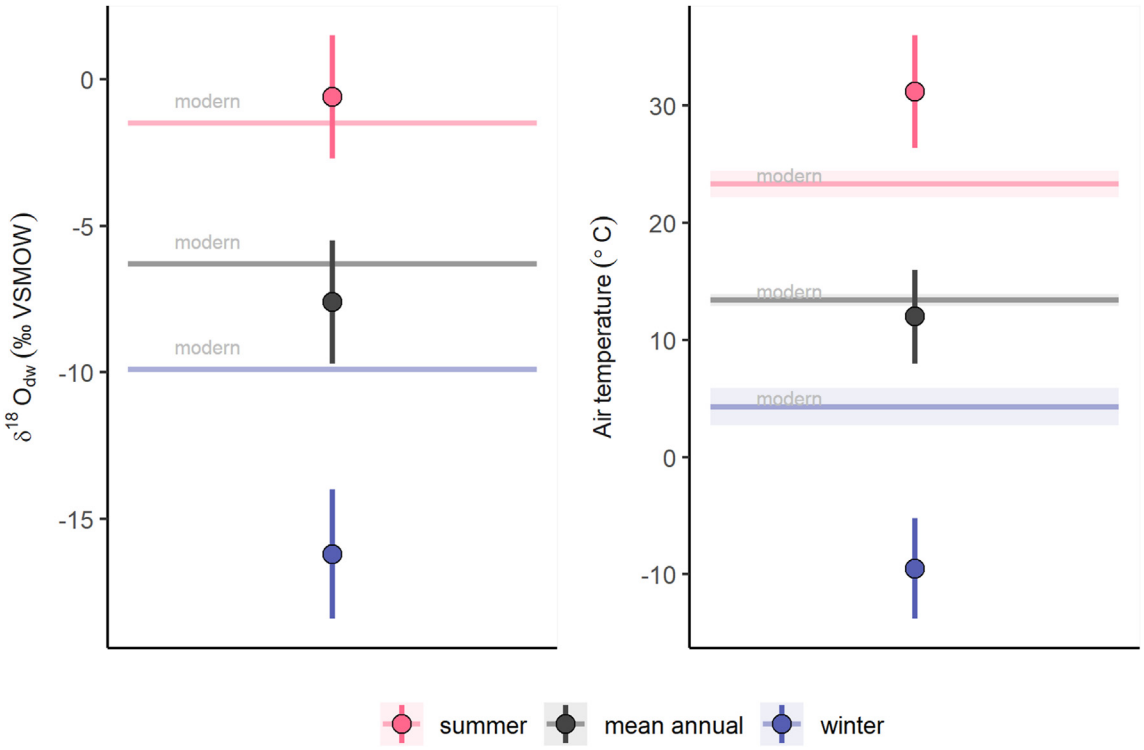

Figure 4. Estimated mean annual, summer, and winter oxygen isotope values of drinking water ($\delta^{18}O_{dw}$) and estimated paleotemperatures for the study site, calculated from archaeological $\delta^{18}O_{enamel}$ data, with associated compound errors shown as error bars. Lines represent modern $\delta^{18}O_{precip}$ data (left) and modern temperatures (right) for the area of the study site, with associated standard deviations shown as shaded ribbons. $\delta^{18}O_{precip}$ data were obtained from the OIPC (Bowen and Revenaugh, 2003; Bowen et al., 2005; Bowen, 2022) and temperature data from the ClimateEU model and averaged for 1981–2009 (Marchi et al., 2020). Abbreviation: VSMOW = Vienna standard mean ocean water.

of using an inverse model to try and remove the effect of time averaging from the tooth enamel mineralization process. Although we believe seasonal temperatures to be particularly relevant to reconstructing environments and human–climate interactions, this limitation means that temperature seasonality can at most be discussed in relatively broad terms, or when supported by direct isotopic comparisons, and we discuss this in more detail in the following sub-section of 4.1 'Comparison with other Late Pleistocene paleoclimate proxy data sets from France'.

The number of individuals analyzed here is relatively small, which increases the uncertainty around paleotemperature estimates. However, both individuals are remarkably similar in their

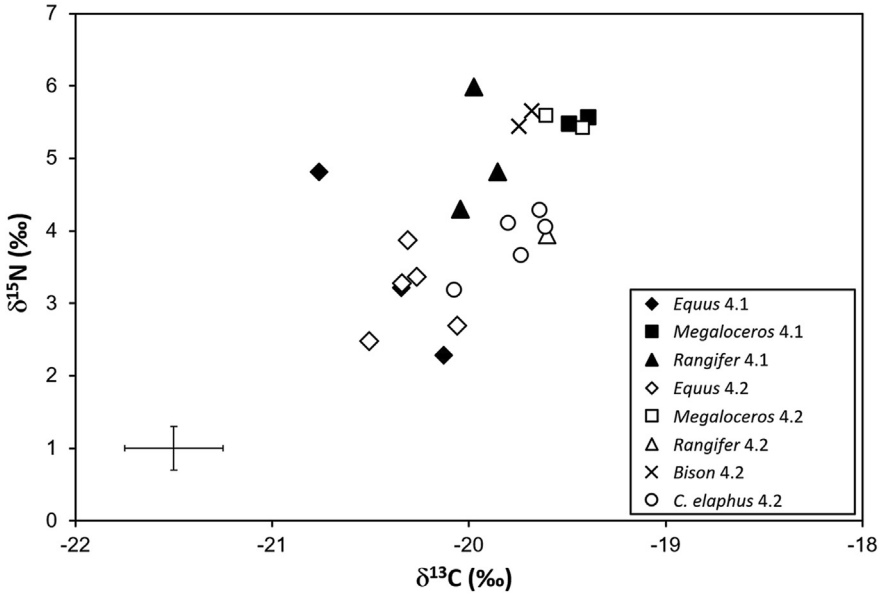

Figure 5. Bivariate plot of $\delta^{13}C$ and $\delta^{15}N$ values of bone collagen from *Bison*, *Cervus elaphus*, *Equus*, *Rangifer*, and *Megaloceros* from Abri du Maras (levels 4.1 and 4.2). Analytical error (±1 SD) is also shown.

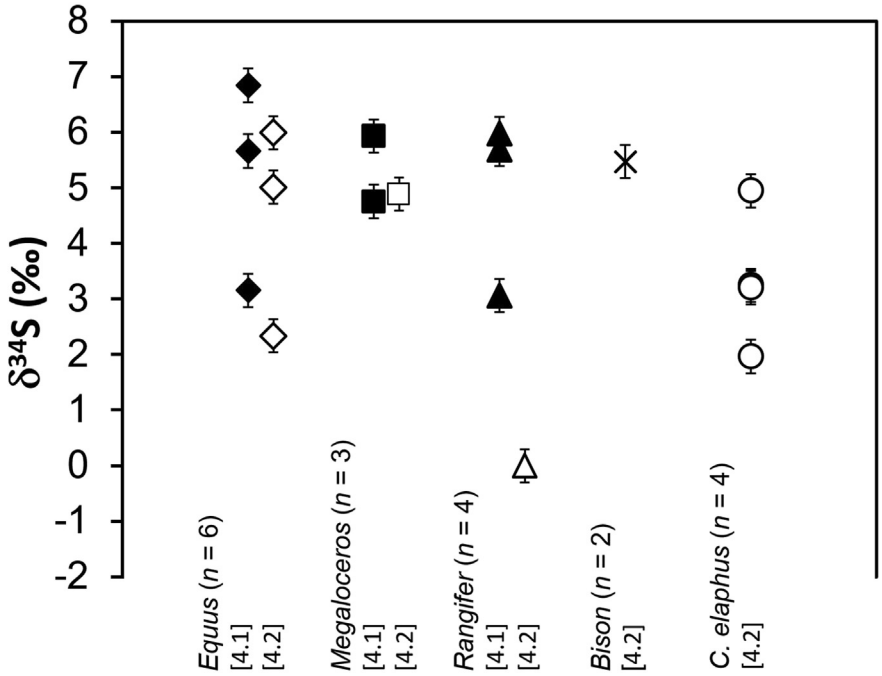

Figure 6. Stable sulfur isotope data of bone collagen from *Bison*, *Cervus elaphus*, *Equus*, *Rangifer*, and *Megaloceros* from Abri du Maras (levels 4.1 and 4.2). Analytical error (±1 SD) is shown.

$\delta^{18}O$ seasonal curves, indicating a consistent reflection of environmental parameters across individuals. At the same time, sinusoidal $\delta^{18}O$ curves with a pronounced seasonal amplitude in both individuals indicate that they were unlikely to have obtained much drinking water from a seasonally buffered water source such as large rivers or springs fed from groundwater. This further indicates that *Equus* at Abri du Maras most likely reflect climatic impacts on $\delta^{18}O$ values of local environmental water sourced from precipitation. Impacts of slight differences in habitat and water source use on enamel $\delta^{18}O$ values between animals drinking water from the Rhône River compared to those drinking precipitation-fed water sources on the local limestone plateaus have been suggested for the data set from Payre (Ecker et al., 2013; Bocherens et al., 2016), a site located on a similar hydrotopographic setting in close proximity to the Rhône ~50 km upstream of Abri du Maras. A similar scenario could potentially also be envisaged for Abri du Maras, which is also situated only a few hundred of meters from the Rhône River. However, the seasonally pronounced $\delta^{18}O$ variation in the level 4.2 horses does not support this. As larger rivers generally exhibit low seasonal $\delta^{18}O$ variability due to higher water residence times, and incorporate snow melt and mixing of water from different locations/altitudes (Rank et al., 2018), a year-round consumption of Rhône River water would most likely result in a lack of seasonal variation in $\delta^{18}O$ values, which is not observed here. Indeed,

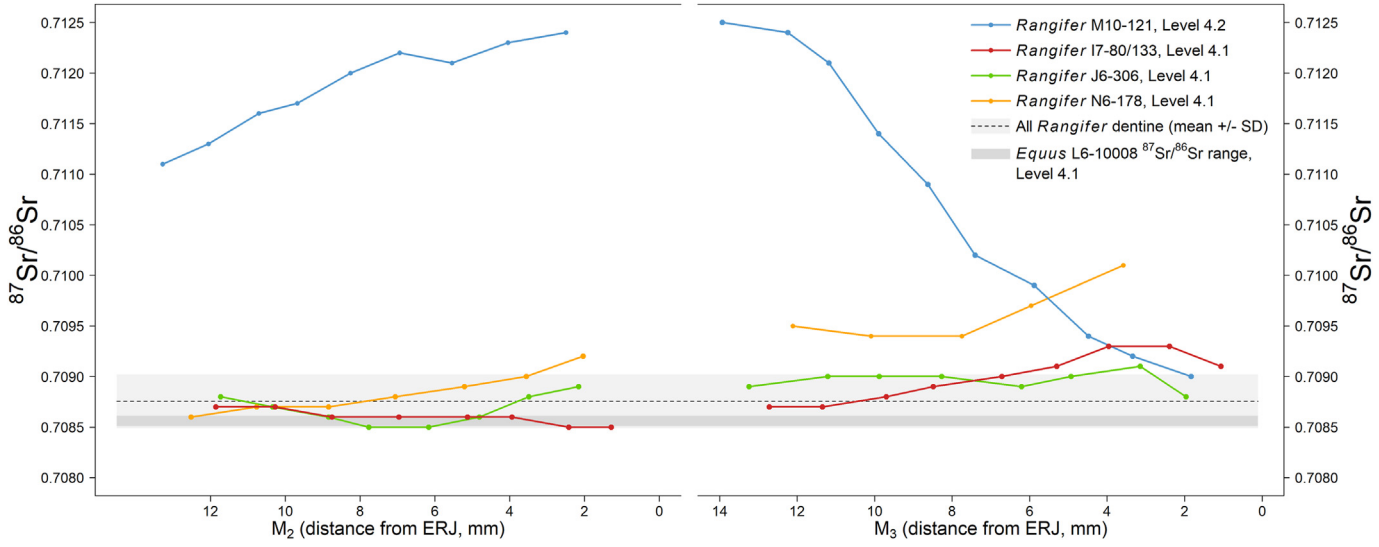

Figure 7. Sequential strontium isotope data from incrementally sampled dental enamel of second and third molars from four *Rangifer* from Abri du Maras. The mean strontium isotope value of dentine sampled is shown (±1 SD) as well as the range of strontium values observed in the third molar of an *Equus* from the site. Analytical error is within the data points. Abbreviation: ERJ = enamel–root junction.

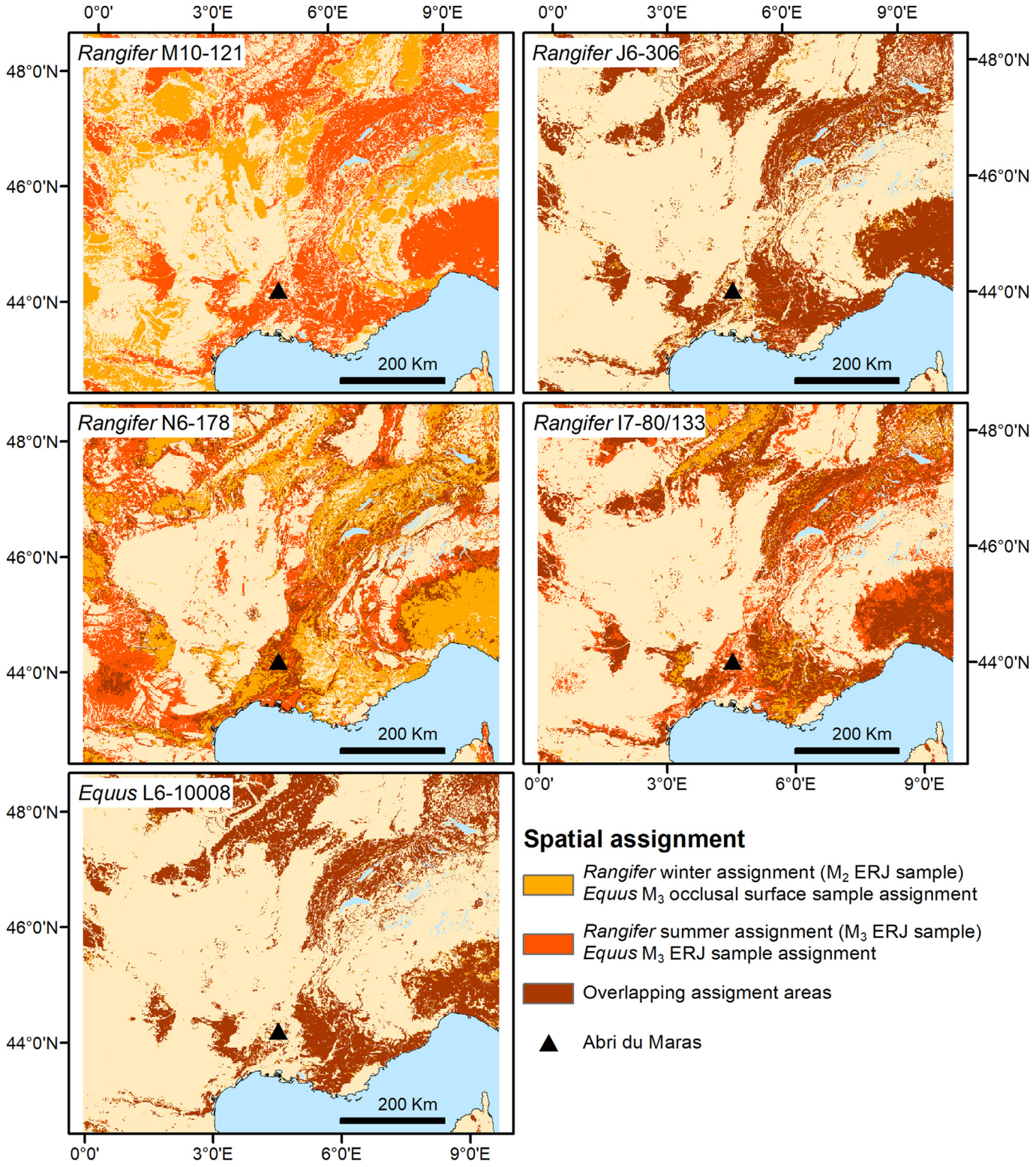

Figure 8. Spatial assignment of strontium isotope data from the enamel sampled closest to the ERJ of the second and third molars of four *Rangifer* (levels 4.1 and 4.2) from Abri du Maras, corresponding broadly to the potential ranges use by the individuals in winter and summer, respectively, based on anticipated enamel mineralization times. Potential seasonal areas correspond to the minimal areas where each sample has 80% chance to originate, and were assessed using the assignR package in R (Ma et al., 2020). Assignments of the samples from close to the occlusal surface and close to the ERJ of the M_3 from one *Equus* are also provided as a reference for an expected local individual. Abbreviation: ERJ = enamel–root junction.

estimates of $\delta^{18}O_{dw}$ show stronger seasonal differences than expected from local precipitation, rather than an attenuated amplitude that could be expected if animals were sourcing from a strongly buffered water source. A substantial contribution of river water to the drinking water of the Abri du Maras *Equus* sampled here therefore seems unlikely, and we instead suggest that their $\delta^{18}O$ values reflect local climatic conditions. This also means that comparatively low winter $\delta^{18}O_{dw}$ values observed in the archaeological specimens compared to modern $\delta^{18}O$ values of precipitation are in our view unlikely to be related to wintertime drinking from low $\delta^{18}O$ river water. Instead, winter may have exhibited more cold/wet conditions compared to today.

Finally, one aspect of the local paleoenvironment that remains unknown and may have had the potential to influence faunal $\delta^{18}O$ values is aridity. High aridity induces ^{18}O-enrichment compared to local precipitation in plants and stagnant open water bodies and therefore in some herbivores, with leaf water or open water signatures superimposing (and therefore obscuring) relationships with precipitation $\delta^{18}O$ values (e.g., Ayliffe and Chivas, 1990; Cormie et al., 1994; Levin et al., 2006). However, in contrast to evaporation-sensitive species (including cervids and caprines), obligate drinkers, such as equids and large bovids, are considered evaporation insensitive and the $\delta^{18}O$ values of their body tissues are unlikely to be strongly influenced by leaf water changes given their dependency on drinking for meeting their water requirements (Levin et al., 2006). At the same time, drinking from evaporatively enriched water bodies such as large lakes, similarly to larger rivers, would result in a lack of seasonal $\delta^{18}O$ variation in animal teeth, which is not observed. It is therefore unlikely the phosphate $\delta^{18}O$ values of the horses included in this study, and the seasonal enrichment observed, is reflecting high aridity. There are few other site-specific indicators of paleoenvironment beyond the faunal suite and isotopic data generated in this study, with the exception of charcoal analysis which has identified wood species including *P. sylvestris* type and *Betula*, the latter of which has been found in level 4.1 (Daujeard et al., 2019; Moncel et al., 2021). While *P. sylvestris* grow in dry and cold conditions, *Betula* require higher soil humidity rates. This may indicate that, in level 4.1 at least, conditions were not overly arid. Future studies at the site could incorporate the oxygen isotope analysis of nonobligate drinking species, such as *C. elaphus*, as a comparison to the obligate drinking species in order to establish water deficiency and, through this, establish an aridity index for the site (e.g., Levin et al., 2006). Future paleoclimatic studies using oxygen isotopes would ideally incorporate strontium isotope analyses, at the very least for serial-samples corresponding to seasonal $\delta^{18}O$ peaks and troughs. Although studies of Late Pleistocene European horses have not indicated migratory behavior (e.g., Pellegrini et al., 2008), and the $^{87}Sr/^{86}Sr$ data from the level 4.1 horse analyzed here are also consistent with sedentary behavior, conservation of this behavior in all phases of the Late Pleistocene cannot be assumed. Furthermore, other species, such as red deer, which could be useful comparators in calculating aridity index, may undertake seasonal movements.

Comparison with other Late Pleistocene paleoclimate proxy data sets from France Owing to the uncertainty inherent in the conversion of oxygen isotope delta values of tooth enamel to drinking water isotope values and paleotemperature estimates, a direct comparison with other enamel $\delta^{18}O$ values of Pleistocene horses represents the most robust way of contextualizing these data (Pryor et al., 2014; Skrzypek et al., 2016). A limited amount of published $\delta^{18}O$ data from *Equus* tooth enamel is available for Late Pleistocene southern France, and not all of this data has been obtained as sequential samples. Out of the published data, results from Abri du Maras level 4.2 most closely resemble bulk sampled MIS 3 data from La Baume de Gigny Cave in the French Jura (Fabre et al., 2011) and Combe Grenal in the Dordogne (Richards et al., 2017; Fig. 9). La Baume de Gigny Cave is located approximately 280 km northeast of Abri du Maras, while Combe Grenal is located ~350 km west of Abri du Maras. At La Baume Gigny Cave, *Equus* tooth enamel from Level VIII exhibits a $\delta^{18}O$ value of 17.2‰, almost identical to the midpoint values from Abri du Maras, although these deposits are somewhat younger than Abri du Maras level 4.2 at ~33 ka (Fabre et al., 2011). Sequentially sampled $\delta^{18}O$ data from a single *Equus* tooth from the immediately underlying but undated Level IX shows similar winter $\delta^{18}O$ values, but comparatively lower summer and mean annual $\delta^{18}O$ values than at Abri du Maras. $\delta^{18}O$ values from Combe Grenal were bulk sampled from tooth fragments of varying lengths from a variety of tooth types, which may contribute to a relatively large scatter of $\delta^{18}O$ values (Richards et al., 2017). Individuals that most closely resemble Abri du Maras level 4.2 stem from Layer 10 (18.1‰), Layer 12 (17.3‰) and Layer 14 (18.1‰), which have been tentatively assigned to early MIS 3. Based on these comparisons, the $\delta^{18}O$ results from Abri du Maras level 4.2 fall comparatively high in the range of published $\delta^{18}O$ values for MIS 3 southern France, with relatively high summer peak values and a comparatively pronounced seasonal summer/winter difference. This may indicate relatively warm mean annual climatic conditions with warm summers, compared to other sites from MIS 3. Oxygen isotope data from *Equus* teeth from the geographically closest site of Payre (Ecker et al., 2013; Bocherens et al., 2016) unfortunately predate the data from Abri du Maras that are discussed here making direct comparison difficult. Predicted phosphate $\delta^{18}O$ values (converted from carbonate $\delta^{18}O$) from samples from Levels D, F, and G at Payre fall noticeably below the results from Abri du Maras (Fig. 9). Given the close spatial proximity to Abri du Maras, it is likely that the *Equus* from Payre either experienced far colder climatic conditions in this region during MIS 6 and earlier (Richard et al., 2021) than those at Abri du Maras during MIS 3, or sourced a larger amount of drinking water from rivers of alpine origin, as was proposed by Ecker et al. (2013) and Bocherens et al. (2016).

To compare the Abri du Maras $\delta^{18}O$ results more extensively to other climatic data, the conversions to paleotemperature estimates must be used, as $\delta^{18}O$ values themselves incorporate species-specific offsets from drinking water (Iacumin et al., 1996; Kohn, 1996). Paleotemperature estimates for annual means are for instance similar to the mean annual temperature estimates of ~9–14 °C generated from *Bison* $\delta^{18}O$ data for Layer 5 of La Ferrassie in the Dordogne (Pederzani et al., 2021). However, summer temperature estimates from Abri du Maras are ~5 °C higher and winter temperatures ~10–15 °C lower than temperature estimates from La Ferrassie. As a consequence, the *Equus* $\delta^{18}O$ data from Abri du Maras seems to indicate stronger summer-winter differences in climate. La Ferrassie Layer 5 is similar in age to Abri du Maras level 4.2 but is located ~350 km west of Abri du Maras and closer to the Atlantic rather than the Mediterranean coast. Climatic differences between the two sites may also stem from slight differences in age, as chronometric dates for both deposits show a considerable uncertainty that is typical for this period. On the other hand, geographic differences in climate and circulation may also play a role. Given that the modern-day climate at both locations is very comparable, this means that either age-related climatic differences are a more likely explanation or that geographic climate gradient between the Dordogne and the Ardèche was more pronounced during MIS 3. While these options are difficult to distinguish based on available data, comparisons with both other Pleistocene data and modern-day climatic data indicate that the *Equus* from Abri du Maras level 4.2 lived in a relatively mild climate in terms of mean annual temperature but with a pronounced seasonal temperature difference. The latter is perhaps of most significance when

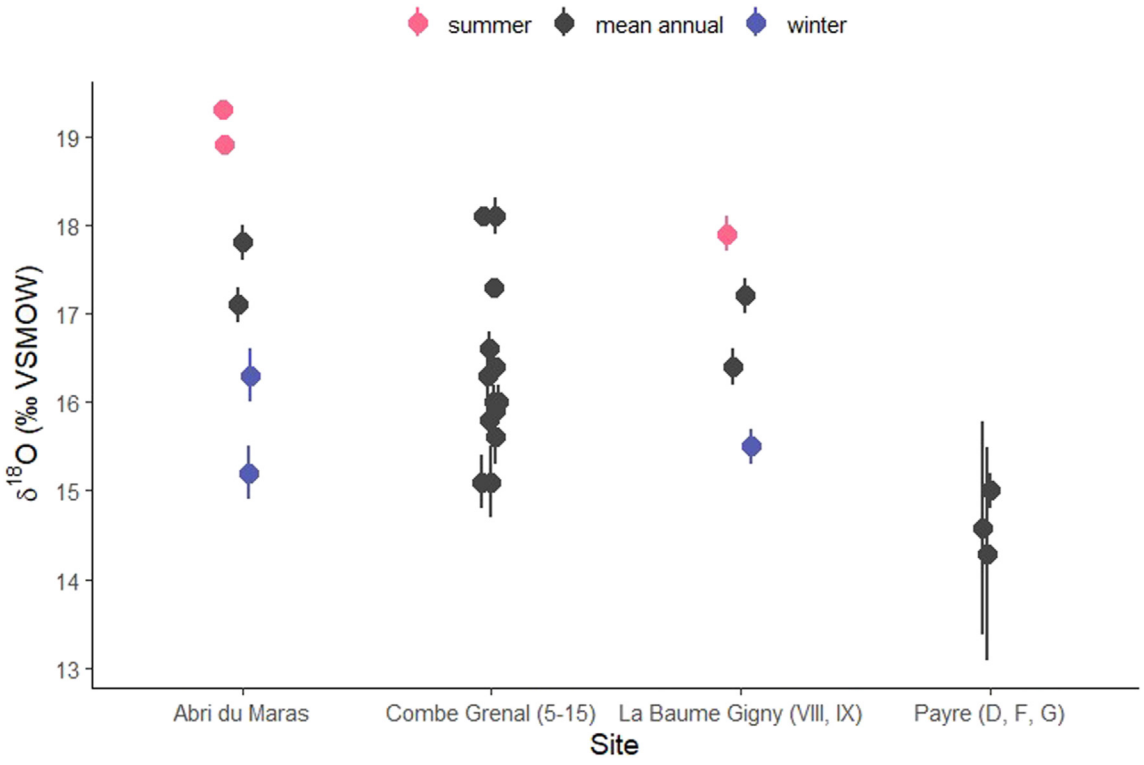

Figure 9. Summer, winter, and mean annual $\delta^{18}O$ data points from Abri du Maras (ADM; Marine Isotope Stage [MIS] 3) level 4.2 exhibit similar values to previously published $\delta^{18}O$ horse enamel data from MIS 3 deposits in southern France (Combe Grenal [CG], La Baume Gigny [BG]), with relatively high summer values and more pronounced seasonality. Values are substantially higher than those reported at the much older site of Payre (MIS 6 and MIS 7–8). Individual data points and error bars represent individual measurements and one standard deviation of replicate measurements (ADM, CG, BG) or Layer means and standard deviations around the mean (Payre, number of teeth per mean are 3, 5, and 6 for levels D, F, and G, respectively). Comparative data were obtained from Fabre et al. (2011; for BG), Richards et al. (2017; for CG), and Ecker et al. (2013; for Payre). Note that the large spread in CG data may be related to the large number of different layers representing MIS 3 at the site, the sampling of unidentified tooth fragments of differing lengths and the relatively uncertain chronology of the site. Abbreviation: VSMOW = Vienna standard mean ocean water.

considering past animal (and human) experience of climate in the region. Seasonal temperature extremes may have impacted the seasonality of Neanderthal landscape use, particularly of higher altitude areas in this region. Indeed, a framework of strong seasonal mobility that has been hypothesized based on archaeological, zooarchaeological, and material culture evidence for this region of southeastern France between the plains of the Rhone Valley and the mid-mountains of the Massif Central from MIS 7 to MIS 3 (Daujeard et al., 2012). However, it must be noted that the seasonal temperature estimations in the present study bear unavoidably large errors of between 4 and 5 °C. Although the lower end of these estimations would still result in cooler winters and warmer summers than are found in the region today, these estimations (and conclusions drawn from them) must be considered with appropriate caution.

4.2. Faunal dietary ecology and broader paleoenvironment

Despite the modest size of the data set, as shown in Figure 5, interspecies differences, particularly in $\delta^{15}N$ values are clear. *Equus* exhibit both the lowest mean $\delta^{13}C$ and $\delta^{15}N$ values. While these values are typical of grazers living in temperate (C3) ecosystems (e.g., Fizet et al., 1995; Bocherens, 2003), given that grasses are normally ^{15}N-enriched relative to shrubs in contemporary arctic and boreal ecosystems (see Bocherens, 2003: 61), it is interesting that the *Bison* are elevated in both $\delta^{15}N$ and $\delta^{13}C$ values relative to *Equus*. These differences are similar to those measured in equids and bovids at the older Eemian site of Neumark-Nord 2, Germany (~126 ka; Britton et al., 2012), and the (broadly) contemporary French site of Marillac (45–40 ka; Fizet et al., 1995). Differences in $\delta^{13}C$ values are likely attributable to differences in the production levels of methane between these different species. Ruminant methane has negative $\delta^{13}C$ values (Metges et al., 1990), potentially leading to tissue enrichment in ^{13}C (e.g., Cerling and Harris, 1999), and similar patterns have been determined in a range of isotopic studies of European Late Pleistocene fauna (see discussion and Britton et al., 2012: Figure 3). However, there is less compelling evidence for a consistent 'offset' in $\delta^{15}N$ values between equids and bovids and the factors influencing $\delta^{15}N$ values in herbivores are complex. Given that modern European bison are mixed/intermediate feeders (Merceron et al., 2014) and shrubs are often depleted in ^{15}N relative to grasses, one may expect collagen $\delta^{15}N$ values of potential mixed feeders should also be lower. However, another factor known to influence collagen $\delta^{15}N$ values of herbivores is the protein content of the diet, with the consumption of higher protein plants leading to increased diet-tissue offsets and ^{15}N-enrichment (Sponheimer et al., 2003). Horses are generally considered to be adapted to live on high-fiber, low-quality forage (Duncan et al., 1990), which could influence diet-tissue offsets and lead to lower $\delta^{15}N$ tissue values. In contrast, the elevated $\delta^{15}N$ values seen in *Bison* here may indicate the incorporation of higher nutrient food such as short grasses, sedges, forbs, and leaves. It should be noted, however, that lower $\delta^{15}N$ values are not always observed in European Pleistocene horses relative to other herbivore species, suggesting that the selection of low-quality forage by horses is not necessarily habitual and may be plastic, shaped by local habitat structure (see discussion in Britton et al., 2012). At Abri du Maras, however, grazing on low-quality forage may indeed account for the

$\delta^{15}N$ values determined in the equids, whereas *Bison* were likely able to feed more flexibly and here are occupying a similar isotopic niche to *Megaloceros*.

At Abri du Maras *Rangifer* $\delta^{13}C$ values are also similar to other intermediate/mixed feeders, including *Bison* and *C. elaphus*. This is unusual as elevated $\delta^{13}C$ values are commonly measured in Pleistocene *Rangifer* compared to other large herbivore taxa and this is often attributed to lichen consumption (e.g., Fizet et al., 1995; Bocherens, 2003), due to the higher $\delta^{13}C$ values observed in modern lichens (e.g., Park and Epstein, 1960; Teeri, 1981). In the Abri du Maras data set, the most elevated $\delta^{13}C$ (and $\delta^{15}N$) values are exhibited in the four *Megaloceros* samples, which are similar both within and between levels. Values exhibited differ from previous isotope studies of pre-LGM *Megaloceros* bone collagen from southwest France which have indicated that this species occupied a similar isotopic niche to *C. elaphus* (Immel et al., 2015), with both taxa exhibiting lower $\delta^{13}C$ values (relative to *Rangifer*) which have been associated with leaf feeding in forested environments, the so-called 'canopy effect' (e.g., Drucker et al., 2008). However, at Abri du Maras differences in $\delta^{13}C$ values between the different cervid species are not as pronounced. There is no indication of a canopy effect in the $\delta^{13}C$ values for either *C. elaphus* or *Megaloceros*, and the similar $\delta^{13}C$ values of the reindeer do not suggest lichen was a major dietary component. The slightly elevated $\delta^{13}C$ values in *Megaloceros* may be related to the consumption of plants such as forb species or sedges, which typically exhibit less negative $\delta^{13}C$ values, as has been concluded for *Megaloceros* dental enamel samples from Ireland (Chritz et al., 2009: 142).

The carbon isotope ratios exhibited in the different deer species at Abri du Maras perhaps reflect the contemporary environmental and ecological suite of this part of France at the time (i.e., that woodland environments may have been mosaic and not extensive/dense). This is consistent with other paleoenvironmental proxy evidence from the site, including charcoal evidence, which is consistent with open forests or forest groves and also with the characterization of mosaic environments in the Rhône Valley and along its tributaries, and other parts of central and southern France, and northern Iberia, during MIS 3 (see discussion in Daujeard et al., 2019). The higher $\delta^{15}N$ values seen in *Megaloceros* at Abri du Maras could also be consistent with this, and the similarity between $\delta^{13}C$ values in *Rangifer*, *Cervus*, and *Megaloceros* may indicate that lichen did not comprise any significant part of *Rangifer* diet in this period and—by inference—that lichen coverage may have been lower during these mild phases (as indicated by the oxygen isotope data from level 4.2 at least). Lichen declines are commonly described in the context of modern global warming and long-term vegetation-specific studies in the Arctic have demonstrated that warmer, and especially more humid conditions, favor mosses and vascular plants and lead to the physiological impairment of lichens and their subsequent decline (Olthof et al., 2008).

When comparing the cervid data from Abri du Maras to that from cooler periods of the Late Pleistocene (e.g., Drucker, 2022), it may be that niche spacing between these species was reduced in this earlier phase of MIS 3. A similar pattern has been seen in deer species during the Lateglacial interstadial and has been attributed to milder and more humid conditions and a decrease in niche partitioning that may have resulted in greater competition between different herbivore species (Immel et al., 2015; Drucker et al., 2018; Drucker, 2022). However, it is important to note that isotopic data do not strictly correspond to niche space but instead to isotopic niche space, and isotopic differences between species are dependent not only on consistently different feeding behaviors but also on the availability of isotopically diverse graze and browse. It may be that in the absence of either dense forest or abundant lichens, carbon isotopic variability in herbivore food sources was reduced overall.

Despite similarities in $\delta^{13}C$ values, a comparatively large range of $\delta^{15}N$ values are shown within and between different species, however (from 2.3‰ to 6.0‰). These likely reflect different feeding behaviors within this environment and, through this, implies local environmental variability in $\delta^{15}N$ values. Multiple factors influence the stable nitrogen isotope ratios of soils and plants and, along with an animal's physiology, can lead to isotopic diversity in animals otherwise occupying the same broader trophic positions (Sponheimer et al., 2003; Szpak, 2014). Bone collagen $\delta^{15}N$ values of large herbivores thus reflect both isotopic variability within local plant communities (which in the past may reflect very different environmental conditions than today) and differences in dietary niche and feeding behavior, the latter of which relates to both the types of plants/plant component consumed (in terms of its isotopic ratio), as well as their nutritional content and digestibility. The range of $\delta^{15}N$ values observed between the different herbivore species at Abri du Maras is evidence for differences in feeding behaviors between taxa. While niche partitioning is commonly seen in other isotope paleoecological studies of herbivores in Western Europe (see reviews in Bocherens, 2003; Drucker, 2022), the data from Abri du Maras highlight that niche feeding behaviors and resource partitioning varied throughout different phases of MIS 3, as well as geographically (e.g., Schwartz-Narbonne et al., 2019; Drucker, 2022). This emphasizes the need to recognize plastic and/or nonanalogous behaviors (and the role of isotope analyses in revealing these) when considering the nonanalogous animal and plant communities of MIS 3 in northern Europe. In the case of Abri du Maras, given that these differences are far less apparent in $\delta^{13}C$ than $\delta^{15}N$ values, the value of combining these two isotopic systems in reconstructing Late Pleistocene herbivore feeding behaviors in particular is also highlighted. Finally, another factor that is not often considered alongside dietary isotopic data in studies of faunal paleoecology but could play a part in the large range of nitrogen isotope values observed in this study could be differences in the habitat use/spatial ecology of different individuals, different species and through time, in this region.

4.3. Evidence for interspecific differences in spatial ecology

Although more than half of the samples (group 1 = 12/19, across all species and both levels) have $\delta^{34}S$ values consistent with anticipated local environmental values (Fig. 6; SOM Fig. S4), six of the remaining seven (group 2) have lower $\delta^{34}S$ values and therefore may have spent a proportion of their lives in a more remote region, and possibly further inland (e.g., along the Rhône Valley where values of ~3‰ can be found). In addition to highlighting potential differences in faunal geographical range, this may also indicate that the resource catchment for the site (i.e., areas from which hominins using the site took prey) went beyond the immediate locale of the site. A further individual, the single *Rangifer* individual from level 4.2 (M10-121), displayed a far lower value than all other samples analyzed, with a value of 0.0‰. This may hint at a very different biogeographical range for this earlier individual compared to the individuals sampled from level 4.1, perhaps far north of the Ardèche region. Indeed, the strontium isotope data from this same individual (see Section 4.4) support this as the likely explanation.

Although two groups are evident in the sulfur isotope data, and the majority do align with predicted local values, it must be borne in mind that sulfur isotope variability in this region in the Late Pleistocene may have been very different compared to more recent periods and could have incorporated lower (or higher) overall environmental $\delta^{34}S$ values. For example, southern France is a region heavily exposed to dust aerosol deposition from the Sahara, one of the main drivers of the $\delta^{34}S$ isoscape, leading to ^{34}S enrichment in the environment (Bataille et al., 2021). The lower values observed for group 2 could be due to differences in dust deposal rates

between the Late Pleistocene and more recent periods as the most recently published sulfur isoscape was established using more recent samples from the Mesolithic to the 20th century (Bataille et al., 2021). A strong correspondence between sulfur isotope values of bone collagen and environmental conditions (in particular, temperature or the extent of permafrost) has also been highlighted by other studies (Drucker et al., 2011; Reade et al., 2020), suggesting that environmental $\delta^{34}S$ not only varies spatially but can vary temporally at the same location. No clear trend in $\delta^{34}S$ values was observed through time between levels 4.1 and 4.2 at Abri du Maras and differences observed between animals therefore likely do reflect relative differences in individual biogeography. However, differences in the presence and extent of permafrost across this mountainous region in the past, or other environmental variables, may have produced a more varied sulfur isoscape compared to the present day that could encompass all the values in this study. Although there may be relative trends, including two statistically distinguishable groups (including a larger group of ungulates of all taxa matching the local predicted values) and an individual reindeer with a distinct $\delta^{34}S$ value compared to all other individuals, given uncertainties surrounding the Late Pleistocene sulfur isoscape, these patterns are difficult to relate to specific geographical areas and in order to explore the biogeography of species more closely (particularly *Rangifer*), strontium isotope data are required.

4.4. Rangifer *migratory behavior at Abri du Maras*

Evidence for plasticity in behavior of *Rangifer* between levels 4.1 and 4.2 The agreement in strontium isotope values in the earliest forming parts of the second molar for the three *Rangifer* from level 4.1 points to a period spent on a similar lithology to one another during the first summer of life (~0.709), consistent with bioavailable strontium isotope values found within ~50 km of the site (including areas on eastern side of the Rhône Valley, and slightly further north; SOM Fig. S7). This may be consistent with the calving grounds and summer range for the *Rangifer* in level 4.1 being relatively close to the site, in the eastern part of the Rhône Valley or even the Prealps area. Strontium isotope ratios from the later forming parts of the second molar (corresponding with the first winter of life) of the three individuals from level 4.1, and values from the majority of their third molars (largely forming in the second year of life), are again similar to one another—albeit with a greater intratooth variation in the third molar between these three individuals compared to the second molar. This is consistent with modern ecological observations and experimental isotope studies on modern herds which show increased dispersals across the herd range during the second half of the first year of life, and into the second year of an animal's life (Britton et al., 2009; Britton, 2010). However, despite slight intratooth variation, values do not deviate considerably or outside of the range of bioavailable strontium within ~50 km of the site and, significantly, do not demonstrate any clear seasonally cyclical trend in the second and/or third molar.

With the exception of a fidelity to calving ground (and thus summer range during the first months of life), the data from level 4.1 *Rangifer* do not suggest regular, targeted seasonal migrations during this period. Potential winter and summer ranges identified from the samples closest to the ERJ in both the M_2 and the M_3 can be found in the vicinity of Abri du Maras and show a substantial overlap and continuity. This range may also have incorporated areas to the east, toward the Prealps, or to the south toward the Mediterranean, although it should be noted that (given the sea-spray effect) the absence of $\delta^{34}S$ values greater than 6‰ may indicate the latter is unlikely. In modern caribou populations, sedentary behavior is observed in the forest and mountain ecotypes (Festa-Bianchet et al., 2011). However, while modern sedentary caribou do not undertake migrations, they may use fairly large home ranges exceeding 1400 km^2, especially where human environmental disturbance is low (Wilson et al., 2019). At Abri du Maras, a nonmigratory ecotype, equivalent to the modern forest ecotype would be consistent with the charcoal analysis in level 4.1, the only level yielding an association of *Betula* and *Pinus*, showing that the environment at the time, was probably humid with open forest or forest groves (Daujeard et al., 2019; Moncel et al., 2021). The $\delta^{13}C$ values from the reindeer and other cervids in this study (see section 4.2), however, make it unlikely that this contemporary woodland would have been extensive (i.e., there is no 'canopy effect'). The strontium isotope values from the single *Equus* sampled from this level and the associated assignment maps are also consistent with living in the region close to the site, at least during the period of formation of this tooth, and may indicate both these species may have been regionally available during much of the year during this later phase of site occupation.

In comparison to the individuals from level 4.1, the intratooth strontium isotope profile of the individual from level 4.2 demonstrates a strong seasonal variability (from lower values to higher values, before a return to lower values). While values in the latest forming parts of the third molar (SOM Fig. S9; *Rangifer* M10-121) do overlap with local biosphere values (and with the values measured in the three *Rangifer* from level 4.1), the values from earlier phases in this individual's life are much higher, particularly in the latest forming parts of the second molar. The complete separation between potential summer and winter ranges inferred from the spatial assignment strongly suggests a migratory behavior. While the potential summer range is very similar to the range used by the individuals from level 4.1, incorporating the area immediately surrounding Abri du Maras, the *Rangifer* from level 4.2 occupied winter areas distinct from the region surrounding the site and completely different from the *Rangifer* from level 4.1. Intratooth values closest to the ERJ in the M_2 of this individual are instead consistent with long-distance movements between the northern and the southern part of the Rhône Valley, or east-west movements, as bioavailable values matching those within the teeth can be found only in excess of 150–200 km from the site. Even areas detected further away, in the southwest France, could be considered as potential winter range habitats, as these are still within the range of distances traveled by modern migratory caribou populations. The distinct sulfur isotope values in the bone collagen of this individual, compared to other herbivores analyzed from the site supports the idea of a distinct total range size, incorporating, perhaps a larger and more (isotopically) diverse area than any of the other animals.

Implications for understanding site and resource use at Abri du Maras These findings provide tentative evidence of differences in ranging behavior in *Rangifer* in the Rhône Valley during MIS 3 and have implications for our understanding of faunal paleoecology and exploitation at Abri du Maras. The data from levels 4.2 and 4.1 infer that both migratory reindeer and less mobile/sedentary ecotypes of reindeer could have been found in Late Pleistocene Europe at this time and/or that this behavior was plastic over time. This was also determined to be the case at Jonzac, where *Rangifer* in Quina Mousterian levels (73 ± 7 ka) were revealed to be migratory using strontium isotope analysis, but that *Rangifer* from Denticulate Mousterian levels (56 ± 3 ka) were likely nonmigratory (Britton, 2010, 2018; Britton et al., 2011).

If the *Rangifer* were indeed nonmigratory in level 4.1 or undertook only very restricted seasonal movements over a small home range, this may suggest that *Rangifer*—like the *Equus*—may have been a year-round local resource at that time in the Rhône Valley. However, the zooarchaeological evidence from this level suggests they were not exploited all year round and instead were hunted exclusively in autumn-winter (Daujeard et al., 2019). This may be consistent with seasonally restricted use of the site by Neanderthals

during the accumulation of deposits in level 4.1. Indeed, a subsistence base centered on strongly seasonal movements has been hypothesized for this region more broadly (Daujeard et al., 2012). Targeted autumn-winter hunting may also be consistent with the deliberate selection of this prey taxa only during peak condition. Autumn is a period where female and young reindeer/caribou in particular are in good physical condition (Miller, 1974), with typically higher average body masses (and body fat percentages) in autumn than in spring and summer (Gerhart et al., 1996; Couturier et al., 2009). Autumn may also have been the optimal period to hunt reindeer for their winter coats (i.e., for clothing; e.g., Binford, 1978; Stenton, 1991; Issenman, 2011). Thus, in the presence of other available local resources—such as horse—reindeer may not have been an appealing option at other points of the year. In contrast, zooarchaeological data from level 4.2 point to a more mixed profile, comprising multiple ungulate species without a strong seasonality. Here, intratooth samples from a single *Rangifer* indicate a seasonally repeating mobility pattern, indicating they may have only been found in the immediate region at certain points of the year (i.e., summer). The investigation of *Rangifer* exploitation, and particularly the seasonality of that exploitation at other sites surrounding Abri du Maras and those sites on the eastern side of the Rhône Valley, may allow the further exploration of the relationship between Neanderthal landscape use and the seasonal biogeography of reindeer.

In addition to the strontium isotope data from the *Rangifer* samples, the results of other analyses undertaken here also have implications for our understanding of Neanderthal activities at the site. The presence of two statistically significant groups revealed by hierarchical cluster analysis of sulfur isotope data may suggest that Neanderthals at the site were extracting their prey from at least two isotopically distinct areas (in terms of $\delta^{34}S$), including locally as well as perhaps further inland along the Rhône Valley. This hints at the potential for isotope zooarchaeological approaches to reveal such aspects of landscape use in subsistence behaviors. However, such a pattern could also be produced through the hunting of animals close to site that had more extensive ranges than others, and thus incorporated a more diverse range of $\delta^{34}S$ values. Further work, incorporating strontium isotope analysis of multiple species would be required to characterize this, ideally in comparison with similar data from other archaeological sites in the region. Comparison with data derived from fauna from nonanthropogenic contexts (e.g., natural accumulations) could be helpful in characterizing variability due to differences in faunal spatial behaviors from variability due to differences in human hunting ranges.

Finally, the oxygen isotope data generated from level 4.2 suggest that, in this phase at least, the climate was comparatively mild for the period, albeit with a pronounced seasonality, with higher and lower seasonal extremes in temperature than experienced in the region today. Based on zooarchaeological data, occupations in level 4.2 at Abri du Maras were restricted to spring-summer, and to autumn (Vignes, 2021). While sample size, and the lack of comparative data from level 4.1 necessitates caution in data interpretation, this may indicate a preference for other sites and/or areas during cooler winter months. The collection of similar data from other sites in the region, combined with site-seasonality data, would help us to better understand the relationship between the seasonal climate and the seasonal use of sites and resources by Neanderthals in the Rhône Valley during MIS 3.

5. Conclusions

The data presented in this article provide evidence for both environmental conditions during MIS 3 in southeastern France, but also for the ecology of key species that Neanderthal groups depended upon. Oxygen isotope analysis of horse teeth from level 4.2 evidence mild climatic conditions, albeit with a seasonality more pronounced than today. Carbon and nitrogen isotope analysis of bone collagen suggests different niche feeding behaviors among herbivore species at the site, mostly expressed through variability in $\delta^{15}N$. Carbon isotope data from *Rangifer* are similar to other taxa studied, which is unusual for Late Pleistocene case studies, particular from later (colder) phases of MIS 3, which indicate that lichens were not making up a significant component of *Rangifer* diet in this area at this time. This may also therefore provide indirect evidence for a lack of contemporary lichen cover, which could be consistent with milder and also moister climatic conditions, notably during level 4.1. Conversely, the $\delta^{13}C$ values from the reindeer and other cervids in this study, however, do not indicate woodland was extensive (i.e. there is no 'canopy effect') and may have been restricted to groves as part of a mosaic environment, which is in agreement with the limited contemporary paleoenvironmental data (Daujeard et al., 2019). The strontium and sulfur isotope data from *Rangifer* provide direct evidence for both migratory and nonmigratory ecotypes at the site, correlating with differences in seasonal exploitation between the two levels. While environmental strontium values surrounding Abri du Maras are most consistent with those observed in the winter-forming parts of *Rangifer* teeth in level 4.1, environmental values matching other periods of the level 4.1 individuals' lives can be found within ~50 km of the site. Thus, in this part of the Rhône Valley, reindeer may have represented a year-round resource. In light of this, we can infer perhaps that the targeted hunting of reindeer in autumn during this phase of site use may be consistent with seasonally-restricted use of the site by Neanderthals and/or the selection of *Rangifer* in prime condition rather than their seasonally restricted availability. In contrast, a single *Rangifer* sampled from level 4.2 demonstrates a very different trend in intratooth strontium and bulk bone collagen sulfur isotope data, suggesting a distinct biogeographical range incorporating other regions and also different seasonal mobility. Data from this individual suggest reindeer may only have been found in the area seasonally (in spring/summer). Thus, the integration of isotope data with the zooarchaeological analyses and other paleoenvironmental proxy data at Abri du Maras evidence not only diversity in animal behavior and ecology during MIS 3, but also demonstrate the inter-relationships between the dynamic ecosystem and Neanderthal land use and hunting strategies. The determination of seasonality of site use and hunting at different archaeological sites in the eastern and western areas of the southern Rhône Valley, combined with further analysis of faunal biogeography and seasonal paleoenvironmental conditions, may help to further illuminate these relationships.

Conflict of interest statement

The authors declare there is no conflict of interest.

Acknowledgments

This research was funded by the Leverhulme Trust (RPG-2017-410 and PLP-2019-284 to K.B.), Muséum National d'Histoire Naturelle, and the Max Planck Society. K.J. thanks ERC Grant ARCHEIS (grant number 803676) and E.L.J. thanks Belspo BRAIN-be ICHIE for salary support during production of this manuscript. Thanks to Ciara Gigleux (Aberdeen), Juan Marin (Muséum National d'Histoire Naturelle), Sven Steinbrenner (MPI-EVA), and Kerry Sayle (SUERC) for assistance during sample selection, preparation, and analysis.

Supplementary Online Material

Supplementary Online Material related to this article can be found at https://doi.org/10.1016/j.jhevol.2022.103292.

References

Ambrose, S.H., 1990. Preparation and characterization of bone and tooth collagen for isotopic analysis. J. Archaeol. Sci. 17, 431–451.

Amundson, R., Austin, A.T., Schuur, E.A.G., Yoo, K., Matzek, V., Kendall, C., Uebersax, A., Brenner, D., Baisden, W.T., 2003. Global patterns of the isotopic composition of soil and plant nitrogen. Global Biogeochem. Cycles 17.

Ayliffe, L., Chivas, A.R., 1990. Oxygen isotope composition of bone phosphate of Australian kangaroos: Potential as a palaeoenvironmental recorder. Geochim. Cosmochim. Acta 54, 2603–2609.

Barron, E., van Andel, T.H., Pollard, D., 2003. Glacial environments II: Reconstructing the climate of Europe in the last glaciation. In: Van Andel, T.H., Davies, W. (Eds.), Neanderthals and Modern Humans in the European Landscape During the Last Glaciation. McDonald Institute for Archaeological Research, Cambridge, pp. 57–78.

Bataille, C.P., Crowley, B.E., Wooller, M.J., Bowen, G.J., 2020. Advances in global bioavailable strontium isoscapes. Palaeogeogr. Palaeoclimatol. Palaeoecol. 555, 109849.

Bataille, C.P., Jaouen, K., Milano, S., Trost, M., Steinbrenner, S., Crubézy, É., Colleter, R., 2021. Triple sulfur-oxygen-strontium isotopes probabilistic geographic assignment of archaeological remains using a novel sulfur isoscape of western Europe. PLoS One 16, e0250383.

Ben-David, M., Shochat, E., Adams, L.G., 2001. Utility of stable isotope analysis in studying foraging ecology of herbivores: Examples from moose and caribou. Alces 37, 421–434.

Bendrey, R., Vella, D., Zazzo, A., Balasse, M., Lepetz, S., 2015. Exponentially decreasing tooth growth rate in horse teeth: Implications for isotopic analyses. Archaeometry 57, 1104–1124.

Bentley, R.A., 2006. Strontium isotopes from the earth to the archaeological skeleton: A review. J. Archaeol. Method Theory 13, 135–187.

Bernard, A., Daux, V., Lécuyer, C., Brugal, J.-P., Genty, D., Wainer, K., Gardien, V., Fourel, F., Jaubert, J., 2009. Pleistocene seasonal temperature variations recorded in the $\delta^{18}O$ of *Bison priscus* teeth. Earth Planet. Sci. Lett. 283, 133–143.

Binford, L.R., 1978. Nunamiut Ethnoarchaeology. Academic Press, New York.

Blumenthal, S.A., Cerling, T.E., Chritz, K.L., Bromage, T.G., Kozdon, R., Valley, J.W., 2014. Stable isotope time-series in mammalian teeth: In situ $\delta^{18}O$ from the innermost enamel layer. Geochim. Cosmochim. Acta 124, 223–236.

Bocherens, H., 2003. Isotopic biogeochemistry and the palaeoecology of the mammoth steppe fauna. DEINSEA Annual of the Natural History Museum Rotterdam 9, 57–76.

Bocherens, H., Díaz-Zorita Bonilla, M., Daujeard, C., Fernandes, P., Raynal, J.-P., Moncel, M.-H., 2016. Direct isotopic evidence for subsistence variability in Middle Pleistocene Neanderthals (Payre, southeastern France). Quat. Sci. Rev. 154, 226–236.

Boethius, A., Ahlström, T., Kielman-Schmitt, M., Kjällquist, M., Larsson, L., 2022. Assessing laser ablation multi-collector inductively coupled plasma mass spectrometry as a tool to study archaeological and modern human mobility through strontium isotope analyses of tooth enamel. Archaeol. Anthropol. Sci. 14, 97.

Bonafini, M., Pellegrini, M., Ditchfield, P., Pollard, A., 2013. Investigation of the 'canopy effect' in the isotope ecology of temperate woodlands. J. Archaeol. Sci. 40, 3926–3935.

Bowen, G.J., 2022. OIPC: The online isotopes in precipitation calculator. Version 3.1. http://waterisotopes.org.

Bowen, G.J., Wassenaar, L., Hobson, K.A., 2005. Global application of stable hydrogen and oxygen isotopes to wildlife forensics. Oecologia 143, 337–348.

Bowen, G.J., Revenaugh, J., 2003. Interpolating the isotopic composition of modern meteoric precipitation. Water Resour. Res. 39, 1–13.

Britton, K., 2010. Multi-isotope analysis and the reconstruction of prey species palaeomigrations and palaeoecology. Ph.D. Dissertation, Durham University.

Britton, K., 2018. Prey species movements and migrations in ecocultural landscapes: Reconstructing late Pleistocene herbivore seasonal spatial behaviours. In: Pilaar-Birch, S. (Ed.), Multi-Species Archaeology. Routledge, London, pp. 347–367.

Britton, K., 2020. Isotope analysis for mobility and climate studies. In: Britton, K., Richards, M. (Eds.), Archaeological Science: An Introduction. Cambridge University Press, Cambridge, pp. 99–124.

Britton, K., Gaudzinski-Windheuser, S., Roebroeks, W., Kindler, L., Richards, M.P., 2012. Stable isotope analysis of well-preserved 120,000-year-old herbivore bone collagen from the Middle Palaeolithic site of Neumark-Nord 2, Germany reveals niche separation between bovids and equids. Palaeogeogr. Palaeoclimatol. Palaeoecol. 333–334, 168–177.

Britton, K., Grimes, V., Dau, J., Richards, M.P., 2009. Reconstructing faunal migrations using intra-tooth sampling and strontium and oxygen isotope analyses: A case study of modern caribou (*Rangifer tarandus granti*). J. Archaeol. Sci. 36, 1163–1172.

Britton, K., Grimes, V., Niven, L., Steele, T., McPherron, S., Soressi, M., Kelly, T.E., Jaubert, J., Hublin, J.-J., Richards, M.P., 2011. Strontium isotope evidence for migration in late Pleistocene Rangifer: Implications for Neanderthal hunting strategies at the Middle Palaeolithic site of Jonzac, France. J. Hum. Evol. 61, 176–185.

Britton, K., Pederzani, S., Kindler, L., Roebroeks, W., Gaudzinski-Windheuser, S., Richards, M.P., Tütken, T., 2019. Oxygen isotope analysis of Equus teeth evidences early Eemian and early Weichselian palaeotemperatures at the Middle Palaeolithic site of Neumark-Nord 2, Saxony-Anhalt, Germany. Quat. Sci. Rev. 226, 106029.

Britton, K., Willmes, M., Moffat, I., Grün, R., Mannino, M.A., Woodward, S., Jaouen, K., 2020. Sampling plants and malacofauna in $^{87}Sr/^{86}Sr$ bioavailability studies: Implications for isoscape mapping and reconstructing of past mobility patterns. Front. Ecol. Evol. 8, 579473.

Brown, W.A.B., Chapman, N.G., 1991. Age assessment of fallow deer (Dama dama): From a scoring scheme based on radiographs of developing permanent molariform teeth. J. Zool. 224, 367–379.

Brown, T.A., Nelson, D.E., Vogel, J.S., Southon, J.R., 1988. Improved collagen extraction by modified Longin method. Radiocarbon 30, 171–177.

Bryant, J.D., Luz, B., Froelich, P.N., 1994. Oxygen isotopic composition of fossil horse tooth phosphate as a record of continental paleoclimate. Palaeogeogr. Palaeoclimatol. Palaeoecol. 107, 303–316.

Capo, R.C., Stewert, B.W., Chadwick, O.A., 1998. Strontium isotopes as tracers of ecosystem processes: Theory and methods. Geoderma 82, 197–225.

Cerling, T.E., Harris, J.M., 1999. Carbon isotope fractionation between diet and bioapatite in ungulate mammals and implications for ecological and paleoecological studies. Oecologia 120, 337–363.

Cerling, T., Harris, J.M., Leakey, M.G., 1999. Browsing and grazing in elephants: The isotope record of modern and fossil proboscideans. Oecologia 120, 364–374.

Chritz, K.L., Dyke, G.J., Zazzo, A., Lister, A.M., Monaghan, N.T., Sigwart, J.D., 2009. Palaeobiology of an extinct Ice Age mammal: Stable isotope and cementum analysis of giant deer teeth. Palaeogeogr. Palaeoclimatol. Palaeoecol. 282, 133–144.

Clark, I., Fritz, P., 1997. Environmental Isotopes in Hydrogeology. Lewis Publishers, New York.

Clement, A.C., Peterson, L.C., 2008. Mechanisms of abrupt climate change of the last glacial period. Rev. Geophys. 46, RG4002.

Collins, M.J., Galley, P., 1998. Towards an optimal method of archaeological collagen extraction: The influence of pH and grinding. Anc. Biomol. 2, 209–222.

Copeland, S.R., Sponheimer, M., le Roux, P.J., Grimes, V., Lee-Thorp, J.A., de Ruiter, D.J., Richards, M.P., 2008. Strontium isotope ratios ($^{87}Sr/^{86}Sr$) of tooth enamel: Comparison of solution and laser ablation multicollector inductively coupled plasma mass spectrometry methods. Rapid Commun. Mass Spectrom. 22, 3187–3194.

Cormie, A.B., Luz, B., Schwarcz, H.P., 1994. Relationship between the hydrogen and oxygen isotopes of deer bone and their use in the estimation of relative humidity. Geochim. Cosmochim. Acta 58, 3439–3449.

Couturier, S., Côté, S.D., Huot, J., Otto, R.D., 2009. Body-condition dynamics in a northern ungulate gaining fat in winter. Can. J. Zool. 87, 367–378.

Dansgaard, W., 1964. Stable isotopes in precipitation. Tellus 16, 436–468.

Daujeard, C., Abrams, G., Germonpré, M., Le Pape, J.-M., Wampach, A., Di Modica, K., Moncel, M.-H., 2016. Neanderthal and animal karstic occupations from southern Belgium and south-eastern France: Regional or common features? Quat. Int. 411, 179–197.

Daujeard, C., Fernandes, P., Guadelli, J.-L., Moncel, M.-H., Santagata, C., Raynal, J.-P., 2012. Neanderthal subsistence strategies in Southeastern France between the plains of the Rhone Valley and the mid-mountains of the Massif Central (MIS 7 to MIS 3). Quat. Int. 252, 32–47.

Daujeard, C., Moncel, M.-H., 2010. On Neanderthal subsistence strategies and land use: A regional focus on the Rhone Valley area in southeastern France. J. Anthropol. Archaeol. 29, 368–391.

Daujeard, C., Vettese, D., Britton, K., Béarez, P., Boulbes, N., Crégut-Bonnoure, E., Desclaux, E., Lateur, N., Pike-Tay, A., Rivals, F., Allué, E., Chacón, M.G., Puaud, S., Richard, M., Courty, M.-A., Gallotti, R., Hardy, B., Bahain, J.J., Falguères, C., Pons-Branchu, E., Valladas, H., Moncel, M.-H., 2019. Neanderthal selective hunting of reindeer? The case study of Abri du Maras (south-eastern France). Archaeol. Anthropol. Sci. 11, 985–1011.

Delgado Huertas, A., Iacumin, P., Longinelli, A., 1997. A stable isotope study of fossil mammal remains from the Paglicci cave, southern Italy, 13 to 33 ka BP: Palaeoclimatological considerations. Chem. Geol. 141, 211–223.

Delgado Huertas, A., Iacumin, P., Stenni, B., Sánchez Chillón, B.S., Longinelli, A., 1995. Oxygen isotope variations of phosphate in mammalian bone and tooth enamel. Geochim. Cosmochim. Acta 59, 4299–4305.

Deniel, C., Pin, C., 2001. Single-stage method for the simultaneous isolation of lead and strontium from silicate samples for isotopic measurements. Anal. Chim. Acta 426, 95–103.

DeNiro, M.J., 1985. Postmortem preservation and alteration of in vivo bone collagen isotope ratios in relation to palaeodietary reconstruction. Nature 317, 806–809.

DeNiro, M.J., Epstein, S., 1978. Influence of diet on the distribution of carbon isotopes in animals. Geochim. Cosmochim. Acta 42, 495–506.

Dettman, D.L., Kohn, M.J., Quade, J., Ryerson, F.J., Ojha, T.P., Hamindullah, S., 2001. Seasonal stable isotope evidence for a strong Asian monsoon throughout the past 10.7 m.y. Geology 29, 31–34.

Discamps, E., Jaubert, J., Bachellerie, F., 2011. Human choices and environmental constraints: Deciphering the variability of large game procurement from Mousterian to Aurignacian times (MIS 5-3) in southwestern France. Quat. Sci. Rev. 30, 2755–2775.

Dobberstein, R.C., Collins, M.J., Craig, O.E., Taylor, G., Penkman, K.E.H., Ritz-Timme, S., 2009. Archaeological collagen: Why worry about collagen diagenesis? Archaeol. Anthropol. Sci. 1, 31–42.

Drucker, D.G., 2022. The isotopic ecology of the mammoth steppe. Annu. Rev. Earth Planet. Sci. 50, 395–418.

Drucker, D., Bocherens, H., Pike-Tay, A., Mariotti, A., 2001. Isotopic tracking of seasonal dietary change in dentine collagen: Preliminary data from modern caribou. Earth Planet. Sci. Lett. 333, 303–309.
Drucker, D.G., Bridault, A., Cupillard, C., Hujic, A., Bocherens, H., 2011. Evolution of habitat and environment of red deer (*Cervus elaphus*) during the Late-glacial and early Holocene in eastern France (French Jura and the western Alps) using multi-isotope analysis ($\delta^{13}C$, $\delta^{15}N$, $\delta^{18}O$, $\delta^{34}S$) of archaeological remains. Quat. Int. 245, 268–278.
Drucker, D.G., Bridault, A., Hobson, K.A., Szuma, E., Bocherens, H., 2008. Can carbon-13 in large herbivores reflect the canopy effect in temperate and boreal ecosystems? Evidence from modern and ancient ungulates. Palaeogeogr. Palaeoclimatol. Palaeoecol. 266, 69–82.
Drucker, D.G., Hobson, K.A., Münzel, S.C., Pike-Tay, A., 2012. Intra-individual variation in stable carbon ($\delta^{13}C$) and nitrogen ($\delta^{15}N$) isotopes in mandibles of modern caribou of Qamanirjuaq (*Rangifer tarandus groenlandicus*) and Banks Island (*Rangifer tarandus pearyi*): Implications for tracing seasonal and temporal changes in diet. Int. J. Osteoarchaeol. 22, 494–504.
Drucker, D.G., Stevens, R.E., Germonpré, M., Sablin, M.V., Péan, S., Bocherens, H., 2018. Collagen stable isotopes provide insights into the end of the mammoth steppe in the central East European plains during the Epigravettian. Quat. Res. 90, 457–469.
Duncan, P., Foose, T.J., Gordon, I.J., Gakahu, C.G., Lloyd, M., 1990. Comparative nutrient extraction from forages by grazing bovids and equids: A test of the nutritional model of equid/bovid competition and coexistence. Oecologia 84, 411–418.
Ecker, M., Bocherens, H., Julien, M.-A., Rivals, F., Raynal, J.-P., Moncel, M.-H., 2013. Middle Pleistocene ecology and Neanderthal subsistence: Insights from stable isotope analyses in Payre (Ardèche, southeastern France). J. Hum. Evol. 65, 363–373.
Evans, J.A., Tatham, S., Chenery, S.R., Chenery, C.A., 2007. Anglo-Saxon animal husbandry techniques revealed though isotope and chemical variations in cattle teeth. Appl. Geochem. 22, 1994–2005.
Fabre, M., Lecuyer, C., Brugal, J.P., Amiot, R., Fourel, F., Martineau, F., 2011. Late Pleistocene climatic change in the French Jura (Gigny) recorded in the delta O-18 of phosphate from ungulate tooth enamel. Quat. Res. 75, 605–613.
Feranec, R.S., 2007. Stable carbon isotope values reveal evidence of resource partitioning among ungulates from modern C_3-dominated ecosystems in North America. Palaeogeogr. Palaeoclimatol. Palaeoecol. 252, 575–585.
Festa-Bianchet, M., Ray, J.C., Boutin, S., Côté, S.D., Gunn, A., 2011. Conservation of caribou (*Rangifer tarandus*) in Canada: An uncertain future. Can. J. Zool. 89, 419–434.
Fizet, M., Mariotti, A., Bocherens, H., Langebadre, B., Vandermeersch, B., Borel, J.P., Bellon, G., 1995. Effect of diet, physiology and climate on carbon and nitrogen stable isotopes of collagen in a late Pleistocene anthropic palaeoecosytem - Marillac, Charente, France. J. Archaeol. Sci. 22, 67–79.
Foury, Y., Desclaux, E., Daujeard, C., Defleur, A., Moncel, M.-H., Raynal, J.-P., 2016. Evolution des faunes de rongeurs en moyenne vallée du Rhône (rive droite, Ardèche, France) au cours du Pléistocène moyen final et du Pléistocène supérieur ancien, du MIS 6 au MIS 4. Quaternaire 27, 55–79.
Fricke, H.C., Clyde, W.C., O'Neil, J.R., 1998. Intra-tooth variations in $\delta^{18}O$ (PO_4) of mammalian tooth enamel as a record of seasonal variations in continental climate variables. Geochim. Cosmochim. Acta 62, 1839–1850.
Fuller, B.T., Fuller, J.L., Sage, N.E., Harris, D.A., O'Connell, T.C., Hedges, R.E.M., 2005. Nitrogen balance and $\delta^{15}N$: Why you're not what you eat during nutritional stress. Rapid Commun. Mass Spectrom. 19, 2497–2506.
Fuller, B.T., Fuller, J.L., Sage, N.E., Harris, D.A., O'Connell, T.C., Hedges, R.E.M., 2004. Nitrogen balance and $\delta^{15}N$: Why you're not what you eat during pregnancy. Rapid Commun. Mass Spectrom. 18, 2889–2896.
Funck, J., Heintzman, P.D., Murray, G.G.R., Shapiro, B., McKinney, H., Huchet, J.-B., Bigelow, N., Druckenmiller, P., Wooller, M.J., 2020. A detailed life history of a Pleistocene steppe bison (*Bison priscus*) skeleton unearthed in Arctic Alaska. Quat. Sci. Rev. 249, 106578.
Gadbury, C., Todd, L., Jahren, A.H., Amundson, R., 2000. Spatial and temporal variations in the isotopic composition of bison tooth enamel from the Early Holocene Hudson-Meng Bone Bed, Nebraska. Palaeogeogr. Palaeoclimatol. Palaeoecol. 157, 79–93.
Gat, J.R., 1980. The isotopes of hydrogen and oxygen in precipitation. In: Fritz, P., Fontes, J.-C. (Eds.), Handbook of Environmental Isotope Geochemistry, vol. 1. Elsevier, Amsterdam, pp. 21–42.
Gaudzinski, S., 2006. Monospecific or species-dominated faunal assemblages during the Middle Paleolithic in Europe. In: Hovers, E., Kuhn, S.L. (Eds.), Transitions before the Transition: Evolution and Stability in the Middle Paleolithic and Middle Stone Age. Springer, New York, pp. 137–147.
Gerhart, K.L., White, R.G., Cameron, R.D., Russell, D.E., 1996. Body composition and nutrient reserves of arctic caribou. Can. J. Zool. 74, 136–146.
Godbout, L., Trudel, M., Irvine, J.R., Wood, C.C., Grove, M.J., Schmitt, A.K., McKeegan, K.D., 2010. Sulfur isotopes in otoliths allow discrimination of anadromous and non-anadromous ecotypes of sockeye salmon (*Oncorhynchus nerka*). Environ. Biol. Fishes 89, 521–532.
Green, D.R., Green, G.M., Colman, A.S., Bidlack, F.B., Tafforeau, P., Smith, T.M., 2017. Synchrotron imaging and Markov Chain Monte Carlo reveal tooth mineralization patterns. PLoS One 12, e0186391.
Green, D.R., Smith, T.M., Green, G.M., Bidlack, F.B., Tafforeau, P., Colman, A.S., 2018. Quantitative reconstruction of seasonality from stable isotopes in teeth. Geochim. Cosmochim. Acta 235, 483–504.
Groot, M., Evans, J., Albarella, U., 2020. Mobility of cattle in the Iron Age and Roman Netherlands. J. Archaeol. Sci. Rep. 32, 102416.
Hardy, B.L., Moncel, M.-H., Daujeard, C., Fernandes, P., Béarez, P., Desclaux, E., Navarro, M.G.C., Puaud, S., Gallotti, R., 2013. Impossible Neanderthals? Making string, throwing projectiles and catching small game during Marine Isotope Stage 4 (Abri du Maras, France). Quat. Sci. Rev. 82, 23–40.
Hardy, B.L., Moncel, M.H., Kerfant, C., Lebon, M., Bellot-Gurlet, L., Mélard, N., 2020. Direct evidence of Neanderthal fibre technology and its cognitive and behavioral implications. Sci. Rep. 10, 4889.
Hedges, R.E.M., Clement, J.G., Thomas, C.D.L., O'Connell, T.C., 2007. Collagen turnover in the adult femoral mid-shaft: Modeled from anthropogenic radiocarbon tracer measurements. Am. J. Phys. Anthropol. 133, 808–816.
Hillson, S., 2005. Teeth, 2nd Ed. Cambridge University Press, Cambridge.
Hobbie, E.A., Högberg, P., 2012. Nitrogen isotopes link mycorrhizal fungi and plants to nitrogen dynamics. New Phytol. 196, 367–382.
Hobbie, E.A., Macko, S.A., Shugart, H.H., 1998. Patterns in N dynamics and N isotopes during primary succession in Glacier Bay, Alaska. Chem. Geol. 152, 3–11.
Hofman-Kamińska, E., Bocherens, H., Borowik, T., Drucker, D.G., Kowalczyk, R., 2018. Stable isotope signatures of large herbivore foraging habitats across Europe. PLoS One 13, e0190723.
Högberg, P., 1997. Tansley Review No. 95 ^{15}N natural abundance in soil-plant systems. New Phytol. 137, 179–203.
Holt, E., Evans, J.A., Madgwick, R., 2021. Strontium ($^{87}Sr/^{86}Sr$) mapping: A critical review of methods and approaches. Earth Sci. Rev. 216, 103593.
Hoppe, K.A., Koch, P.L., Carlson, R.W., Webb, D.S., 1999. Tracking mammoths and mastodons: Reconstruction of migratory behaviour using strontium isotope ratios. Geology 27, 439–442.
Hoppe, K.A., Stover, S.M., Pascoe, J.R., Amundson, R., 2004. Tooth enamel biomineralization in extant horses: Implications for isotopic microsampling. Palaeogeogr. Palaeoclimatol. Palaeoecol. 206, 355–365.
Houlton, B.Z., Bai, E., 2009. Imprint of denitrifying bacteria on the global terrestrial biosphere. Proc. Natl. Acad. Sci. USA 106, 21713–21716.
Iacumin, P., Bocherens, H., Mariotti, A., Longinelli, A., 1996. Oxygen isotope analyses of co-existing carbonate and phosphate in biogenic apatite: A way to monitor diagenetic alteration of bone phosphate? Earth Planet. Sci. Lett. 142, 1–6.
Immel, A., Drucker, D.G., Bonazzi, M., Jahnke, T.K., Münzel, S.C., Schuenemann, V.J., Herbig, A., Kind, C.-J., Krause, J., 2015. Mitochondrial genomes of giant deers suggest their late survival in Central Europe. Sci. Rep. 5, 10853.
Issenman, B.K., 2011. Sinews of Survival: The Living Legacy of Inuit Clothing. UBC Press, Vancouver.
Jones, J.R., Richards, M.P., Reade, H., de Quirós, F.B., Marín-Arroyo, A.B., 2019. Multi-isotope investigations of ungulate bones and teeth from El Castillo and Covalejos caves (Cantabria, Spain): Implications for paleoenvironment reconstructions across the Middle-Upper Palaeolithic transition. J. Archaeol. Sci. Rep. 23, 1029–1042.
Jones, J.R., Richards, M.P., Straus, L.G., Reade, H., Altuna, J., Mariezkurrena, K., Marín-Arroyo, A.B., 2018. Changing environments during the Middle-Upper Palaeolithic transition in the eastern Cantabrian Region (Spain): Direct evidence from stable isotope studies on ungulate bones. Sci. Rep. 8, 14842.
Kahlke, R.-D., 2014. The origin of Eurasian Mammoth Faunas (*Mammuthus–Coelodonta* Faunal Complex). Quat. Sci. Rev. 96, 32–49.
Kindler, P., Guillevic, M., Baumgartner, M.F., Schwander, J., Landais, A., Leuenberger, M., 2014. Temperature reconstruction from 10 to 120 kyr b2k from the NGRIP ice core. Clim. Past 10, 887–902.
Koch, P.L., Heisinger, J., Moss, C., Carlson, R.W., Fogel, M.L., Behrensmeyer, A.K., 1995. Isotopic tracking of change in diet and habitat use in African Elephants. Science 267, 1340–1343.
Kohn, M.J., 1996. Predicting animal $\delta^{18}O$: Accounting for diet and physiological adaptation. Geochim. Cosmochim. Acta 60, 4811–4829.
Kohn, M.J., 2004. Comment: Tooth enamel mineralization in ungulates: Implications for recovering a primary isotopic time-series, by B. H. Passey and T. E. Cerling (2002). Geochim. Cosmochim. Acta 68, 403–405.
Kohn, M.J., Schoeninger, M.J., Valley, J.W., 1996. Herbivore tooth oxygen isotope compositions: Effects of diet and physiology. Geochim. Cosmochim. Acta 60, 3889–3896.
Kohn, M.J., Schoeninger, M.J., Valley, J.W., 1998. Variability in oxygen isotope compositions of herbivore teeth: Reflections of seasonality or developmental physiology? Chem. Geol. 152, 97–112.
Kovács, J., Moravcová, M., Újvári, G., Pintér, A.G., 2012. Reconstructing the paleoenvironment of East Central Europe in the Late Pleistocene using the oxygen and carbon isotopic signal of tooth in large mammal remains. Quat. Int. 276, 145–154.
Kuntz, D., Costamagno, S., 2011. Relationships between reindeer and man in southwestern France during the Magdalenian. Quat. Int. 238, 12–24.
Lazzerini, N., Balter, V., Coulon, A., Tacail, T., Marchina, C., Lemoine, M., Bayarkhuu, N., Turbat, T., Lepetz, S., Zazzo, A., 2021. Monthly mobility inferred from isoscapes and laser ablation strontium isotope ratios in caprine tooth enamel. Sci. Rep. 11, 2277.
Legendre, P., Legendre, L., 1998. Numerical Ecology. Elsevier, Amsterdam.
Levin, N.E., Cerling, T.E., Passey, B.H., Harris, J.M., Ehleringer, J.R., 2006. A stable isotope aridity index for terrestrial environments. Proc. Natl. Acad. Sci. USA 103, 11201–11205.
Levinson, A.A., Luz, B., Kolodny, Y., 1987. Variations in oxygen isotopic compositions of human teeth and urinary stones. Appl. Geochem. 2, 367–371.

Lisiecki, L.E., Raymo, M.E., 2005. A Pliocene-Pleistocene stack of 57 globally distributed benthic $\delta^{18}O$ records. Paleoceanography 20, PA1003.
Longin, R., 1971. New method of collagen extraction for radiocarbon dating. Nature 230, 241–242.
Longinelli, A., 1984. Oxygen isotopes in mammal bone phosphate: A new tool for paleohydrological and paleoclimatological research? Geochim. Cosmochim. Acta 48, 385–390.
Luz, B., Kolodny, Y., Horowitz, M., 1984. Fractionation of oxygen isotopes between mammalian bone-phosphate and environmental drinking water. Geochim. Cosmochim. Acta 48, 1689–1693.
Ma, C., Vander Zanden, H.B., Wunder, M.B., Bowen, G.J., 2020. assignR: An R package for isotope-based geographic assignment. Methods Ecol. Evol. 11, 996–1001.
MacFadden, B.J., 2008. Geographic variation in diets of ancient populations of 5-million-year-old (early Pliocene) horses from southern North America. Palaeogeogr. Palaeoclimatol. Palaeoecol. 266, 83–94.
Maguas, C., Brugnoli, E., 1996. Spatial variation in carbon isotope discrimination across the thalli of several lichen species. Plant Cell Environ. 19, 437–446.
Marchi, M., Castellanos-Acuña, D., Hamann, A., Wang, T., Ray, D., Menzel, A., 2020. ClimateEU, scale-free climate normals, historical time series, and future projections for Europe. Sci. Data 7, 428.
Marín, J., Daujeard, C., Saladié, P., Rodríguez-Hidalgo, A., Vettese, D., Rivals, F., Boulbes, N., Crégut-Bonnoure, E., Lateur, N., Gallotti, R., Arbez, L., Puaud, S., Moncel, M.-H., 2020. Neanderthal faunal exploitation and settlement dynamics at the Abri du Maras, level 5 (south-eastern France). Quat. Sci. Rev. 243, 106472.
Mekota, A.M., Grupe, G., Ufer, S., Cuntz, U., 2006. Serial analysis of stable nitrogen and carbon isotopes in hair: Monitoring starvation and recovery phases of patients suffering from anorexia nervosa. Rapid Commun. Mass Spectrom. 20, 1604–1610.
Merceron, G., Hofman-Kamińska, E., Kowalczyk, R., 2014. 3D dental microwear texture analysis of feeding habits of sympatric ruminants in the Białowieża Primeval Forest, Poland. For. Ecol. Manag. 328, 262–269.
Metges, C., Kempe, K., Schmidt, H.-L., 1990. Dependence of the carbon-isotope contents of breath carbon dioxide, milk, serum and rumen fermentation products on the $\delta^{13}C$ value of food in dairy cows. Br. J. Nutr. 63, 187–196.
Miller, F.L., 1974. Biology of the Kaminuriak population of barren-ground caribou. Part 2. Dentition as an indicator of age and sex; composition and socialization of the population. Can. Wildl. Serv. Rep. 31, 1–87.
Moncel, M.-H., Chacón, M.G., La Porta, A., Fernandes, P., Hardy, B., Gallotti, R., 2014. Fragmented reduction processes: Middle Palaeolithic technical behaviour in the Abri du Maras shelter, southeastern France. Quat. Int. 350, 180–204.
Moncel, M.-H., Chacón, M.G., Vettese, D., Courty, M.-A., Daujeard, C., Eixea, A., Fernandes, P., Allué, E., Hardy, B., Rivals, F., Béarez, P., Gallotti, R., Puaud, S., 2021. Late Neanderthal short-term and specialized occupations at the Abri du Maras (South-East France, level 4.1, MIS 3). Archaeol. Anthropol. Sci. 13, 45.
Moncel, M.-h., Daujeard, C., 2012. The variability of the Middle Palaeolithic on the right bank of the Middle Rhône Valley (southeast France): Technical traditions or functional choices? Quat. Int. 247, 103–124.
Nadelhoffer, K., Shaver, G., Fry, B., Giblin, A., Johnson, L., McKane, R., 1996. ^{15}N natural abundances and N use by tundra plants. Oecologia 107, 386–394.
Nehlich, O., 2015. The application of sulphur isotope analyses in archaeological research: A review. Earth Sci. Rev. 142, 1–17.
Nehlich, O., Richards, M.P., 2009. Establishing collagen quality criteria for sulphur isotope analysis of archaeological bone collagen. Archaeol. Anthropol. Sci. 1, 59–75.
Nielsen, H., 1974. Isotopic composition of the major contributors to atmospheric sulfur. Tellus 26, 213–221.
Olthof, I., Pouliot, D., Latifovic, R., Chen, W., 2008. Recent (1986-2006) vegetation-specific NDVI trends in northern Canada from satellite data. Arctic 61, 381–394.
O'Neil, J.R., Roe, L., Reinhard, E., Blake, R.E., 1994. A rapid and precise method of oxygen isotope analysis of biogenic phosphate. Isr. J. Earth Sci. 43, 203–212.
Park, R., Epstein, S., 1960. Carbon isotope fractionation during photosynthesis. Geochim. Cosmochim. Acta 21, 110–126.
Passey, B.H., Cerling, T.E., 2002. Tooth enamel mineralization in ungulates: Implications for recovering a primary isotopic time-series. Geochim. Cosmochim. Acta 66, 3225–3234.
Passey, B.H., Cerling, T.E., Schuster, G.T., Robinson, T.F., Roeder, B.L., Krueger, S.K., 2005. Inverse methods for estimating primary input signals from time-averaged isotope profiles. Geochim. Cosmochim. Acta 69, 4101–4116.
Pederzani, S., Aldeias, V., Dibble, H.L., Goldberg, P., Hublin, J.-J., Madelaine, S., McPherron, S.P., Sandgathe, D., Steele, T.E., Turq, A., Britton, K., 2021. Reconstructing Late Pleistocene paleoclimate at the scale of human behavior: An example from the Neandertal occupation of La Ferrassie (France). Sci. Rep. 11, 1419.
Pederzani, S., Britton, K., 2019. Oxygen isotopes in bioarchaeology: Principles and applications, challenges and opportunities. Earth Sci. Rev. 188, 77–107.
Pellegrini, M., Donahue, R.E., Chenery, C., Evans, J., Lee-Thorp, J., Montgomery, J., Mussi, M., 2008. Faunal migration in late-glacial central Italy: Implications for human resource exploitation. Rapid Commun. Mass Spectrom. 22, 1714–1726.
Peterson, B.J., Fry, B., 1987. Stable isotopes in ecosystem studies. Annu. Rev. Ecol. Evol. Syst. 18, 293–320.
Price, T.D., Meiggs, D., Weber, M.-J., Pike-Tay, A., 2017. The migration of Late Pleistocene reindeer: Isotopic evidence from northern Europe. Archaeol. Anthropol. Sci. 9, 371–394.
Pryor, A.J.E., Stevens, R.E., O'Connell, T.C., Lister, J.R., 2014. Quantification and propagation of errors when converting vertebrate biomineral oxygen isotope data to temperature for palaeoclimate reconstruction. Palaeogeogr. Palaeoclimatol. Palaeoecol. 412, 99–107.
Puzachenko, A.Y., Titov, V.V., Kosintsev, P.A., 2020. Evolution of the European regional large mammals assemblages in the end of the Middle Pleistocene — The first half of the Late Pleistocene (MIS 6–MIS 4). Quat. Int. 20, 155–191.
Rank, D., Wyhlidal, S., Schott, K., Weigand, S., Oblin, A., 2018. Temporal and spatial distribution of isotopes in river water in Central Europe: 50 years experience with the Austrian network of isotopes in rivers. Isotopes Environ. Health Stud. 54, 115–136.
R Core Team, 2021. R: A Language and Environment for Statistical Computing. R Foundation for Statistical Computing, Vienna, Austria. https://www.r-project.org/.
Reade, H., Stevens, R.E., Barker, G., O'Connell, T.C., 2015. Tooth enamel sampling strategies for stable isotope analysis: Potential problems in cross-method data comparisons. Chem. Geol. 404, 126–135.
Reade, H., Tripp, J.A., Charlton, S., Grimm, S.B., Leesch, D., Müller, W., Sayle, K.L., Fensome, A., Higham, T.F.G., Barnes, I., Stevens, R.E., 2020. Deglacial landscapes and the Late Upper Palaeolithic of Switzerland. Quat. Sci. Rev. 239, 106372.
Rendu, W., Costamagno, S., Meignen, L., Soulier, M.-C., 2012. Monospecific faunal spectra in Mousterian contexts: Implications for social behavior. Quat. Int. 247, 50–58.
Richard, M., Falguères, C., Pons-Branchu, E., Bahain, J.J., Voinchet, P., Lebon, M., Valladas, H., Dolo, J.M., Puaud, S., Rué, M., Daujeard, C., Moncel, M.H., Raynal, J.P., 2015. Contribution of ESR/U-series dating to the chronology of late Middle Palaeolithic sites in the middle Rhône valley, southeastern France. Quat. Geochronol. 30, 529–534.
Richard, M., Pons-Branchu, E., Genuite, K., Jaillet, S., Joannes-Boyau, R., Wang, N., Genty, D., Cheng, H., Price, G.J., Pierre, M., Dapoigny, A., Falguères, C., Tombret, O., Voinchet, P., Bahain, J.-J., Moncel, M.-H., 2021. Timing of Neanderthal occupations in the southeastern margins of the Massif Central (France): A multi-method approach. Quat. Sci. Rev. 273, 107241.
Richards, M.P., Fuller, B.T., Hedges, R.E.M., 2001. Sulphur isotopic variation in ancient bone collagen from Europe: Implications for human palaeodiet, residence mobility, and modern pollutant studies. Earth Planet. Sci. Lett. 191, 185–190.
Richards, M.P., Hedges, R.E.M., 2003. Variations in bone collagen delta C-13 and delta N-15 values of fauna from Northwest Europe over the last 40 000 years. Palaeogeogr. Palaeoclimatol. Palaeoecol. 193, 261–267.
Richards, M.P., Pellegrini, M., Niven, L., Nehlich, O., Dibble, H., Turq, A., McPherron, S.J.P., 2017. Temporal variations in *Equus* tooth isotope values (C, N, O) from the Middle Paleolithic site of Combe Grenal, France (ca. 150,000 to 50,000BP). J. Archaeol. Sci. Rep. 14, 189–198.
Ruebens, K., Sinet-Mathiot, V., Talamo, S., Smith, G.M., Welker, F., Hublin, J.-J., McPherron, S.P., 2022. The Late Middle Palaeolithic Occupation of Abri du Maras (Layer 1, Neronian, Southeast France): Integrating lithic analyses, ZooMS and radiocarbon dating to reconstruct Neanderthal hunting behaviour. J. Paleolit. Archaeol. 5, 4.
Sayle, K.L., Brodie, C.R., Cook, G.T., Hamilton, W.D., 2019. Sequential measurement of $\delta^{15}N$, $\delta^{13}C$ and $\delta^{34}S$ values in archaeological bone collagen at the Scottish Universities Environmental Research Centre (SUERC): A new analytical frontier. Rapid Commun. Mass Spectrom. 33, 1258–1266.
Sánchez Chillón, B., Alberdi, M.T., Leone, G., Bonadonna, F.P., Stenni, B., Longinelli, A., 1994. Oxygen isotopic composition of fossil equid tooth and bone phosphate: An archive of difficult interpretation. Palaeogeogr. Palaeoclimatol. Palaeoecol. 107, 317–328.
Schoeninger, M.J., DeNiro, M.J., 1984. Nitrogen and carbon isotopic composition of bone collagen from marine and terrestrial animals. Geochim. Cosmochim. Acta 48, 625–639.
Schwartz-Narbonne, R., Longstaffe, F.J., Kardynal, K.J., Druckenmiller, P., Hobson, K.A., Jass, C.N., Metcalfe, J.Z., Zazula, G., 2019. Reframing the mammoth steppe: Insights from analysis of isotopic niches. Quat. Sci. Rev. 215, 1–21.
Sharp, Z.D., Cerling, T.E., 1998. Fossil isotope records of seasonal climate and ecology: Straight from the horse's mouth. Geology 26, 219–222.
Sjögersten, S., Kuijper, D.P.J., van der Wal, R., Loonen, M.J.J.E., Huiskes, A.H.L., Woodin, S.J., 2010. Nitrogen transfer between herbivores and their forage species. Polar Biol. 33, 1195–1203.
Skrzypek, G., Sadler, R., Wiśniewski, A., 2016. Reassessment of recommendations for processing mammal phosphate $\delta^{18}O$ data for paleotemperature reconstruction. Palaeogeogr. Palaeoclimatol. Palaeoecol. 446, 162–167.
Skrzypek, G., Wiśniewski, A., Grierson, P.F., 2011. How cold was it for Neanderthals moving to Central Europe during warm phases of the last glaciation? Quat. Sci. Rev. 30, 481–487.
Smith, A.B., Epstein, S., 1971. Two categories of $^{13}C/^{12}C$ ratios for higher plants. Plant Physiol. 47, 380–384.
Sponheimer, M., Robinson, T., Ayliffe, L., Roeder, B., Hammer, J., Passey, B., West, A., Cerling, T., Dearing, D., Ehleringer, J., 2003. Nitrogen isotopes in mammalian herbivores: Hair $\delta^{15}N$ values from a controlled feeding study. Int. J. Osteoarchaeol. 13, 80–87.
Stenton, D.R., 1991. The adaptive significance of caribou winter clothing for arctic hunter-gatherers. Études Inuit Stud. 15, 3–28.
Stevens, R.E., Hedges, R.E.M., 2004. Carbon and nitrogen stable isotope analysis of northwest European horse bone and tooth collagen, 40,000 BP-present: Palaeoclimatic interpretations. Quat. Sci. Rev. 23, 977–991.
Stevens, R.E., Jacobi, R., Street, M., Germonpre, M., Conard, N.J., Munzel, S.C., Hedges, R.E.M., 2008. Nitrogen isotope analyses of reindeer (*Rangifer tarandus*),

45,000 BP to 900 BP: Palaeoenvironmental reconstructions. Palaeogeogr. Palaeoclimatol. Palaeoecol. 262, 32–45.
Stewart, J.R., 2005. The ecology and adaptation of Neanderthals during the non-analogue environment of Oxygen Isotope Stage 3. Quat. Int. 137, 35–46.
Szpak, P., 2014. Complexities of nitrogen isotope biogeochemistry in plant-soil systems: Implications for the study of ancient agricultural and animal management practices. Front. Plant Sci. 5, 288.
Teeri, J.A., 1981. Stable carbon isotope analysis of mosses and lichens growing in xeric and moist habitats. Bryologist 84, 82–84.
Trayler, R.B., Kohn, M.J., 2017. Tooth enamel maturation reequilibrates oxygen isotope compositions and supports simple sampling methods. Geochim. Cosmochim. Acta 198, 32–47.
Tütken, T., Vennemann, T.W., Janz, H., Heizmann, H.E.P., 2006. Palaeoenvironment and palaeoclimate of the Middle Miocene lake in the Steinheim basin, SW Germany, a reconstruction from C, O, and Sr isotopes of fossil remains. Palaeogeogr. Palaeoclimatol. Palaeoecol. 241, 457–491.
van Klinken, G.J., 1999. Bone collagen quality indicators for palaeodietary and radiocarbon measurements. J. Archaeol. Sci. 26, 687–695.
Vettese, D., Borel, A., Blasco, R., Chevillard, L., Stavrova, T., Thun Hohenstein, U., Arzarello, M., Moncel, M.-H., Daujeard, C., 2022. New evidence of Neandertal butchery traditions through the marrow extraction in southwestern Europe (MIS 5–3). PLoS One 17, e0271816.
Vignes, M.-P., 2021. Approche multidisciplinaire des stratégies de subsistance des Néandertaliens à l'Abri du Maras (Ardèche): Archéozoologie, taphonomie et analyse spatiale de la grande faune du niveau 4.2 (MIS 3). M.Sc. Dissertation, Muséum national d'Histoire naturelle.
Voelker, A.H.L., 2002. Global distribution of centennial-scale records for Marine Isotope Stage (MIS) 3: A database. Quat. Sci. Rev. 21, 1185–1212.
Wilson, K.S., Pond, B.A., Brown, G.S., Schaefer, J.A., 2019. The biogeography of home range size of woodland caribou Rangifer tarandus caribou. Divers. Distrib. 25, 205–216.
Wißing, C., Rougier, H., Baumann, C., Comeyne, A., Crevecoeur, I., Drucker, D.G., Gaudzinski-Windheuser, S., Germonpré, M., Gómez-Olivencia, A., Krause, J., Matthies, T., Naito, Y.I., Posth, C., Semal, P., Street, M., Bocherens, H., 2019. Stable isotopes reveal patterns of diet and mobility in the last Neandertals and first modern humans in Europe. Sci. Rep. 9, 4433.
Wooller, M.J., Bataille, C., Druckenmiller, P., Erickson, G.M., Groves, P., Haubenstock, N., Howe, T., Irrgeher, J., Mann, D., Moon, K., Potter, B.A., Prohaska, T., Rasic, J., Reuther, J., Shapiro, B., Spaleta, K.J., Willis, A.D., 2021. Lifetime mobility of an Arctic woolly mammoth. Science 373, 806–808.
Wu, J.P., Veitch, A., Checkley, S., Dobson, H., Kutz, S.J., 2012. Linear enamel hypoplasia in caribou (*Rangifer tarandus groenlandicus*): A potential tool to assess population health. Wildl. Soc. Bull. 36, 554–560.
Yurtsever, Y., 1975. Worldwide survey of stable isotopes in precipitation, Report of the Isotope Hydrology Section. International Atomic Energy Agency, Vienna.
Zazzo, A., Lécuyer, C., Mariotti, A., 2004. Experimentally-controlled carbon and oxygen isotope exchange between bioapatites and water under inorganic and microbially mediated conditions. Geochim. Cosmochim. Acta 68, 1–12.
Zazzo, A., Monahan, F.J., Moloney, A.P., Green, S., Schmidt, O., 2011. Sulphur isotopes in animal hair track distance to sea. Rapid Commun. Mass Spectrom. 25, 2371–2378.